



*An-Najah  
National University*

*Faculty of Graduate Studies  
Physics Department*

# **THE MAGNETIC PROPERTIES OF THE ALLOYS Fe(Al,Mn) SYSTEM**

**BY  
Sabri Ahmed Al-Tannah**

**Supervisor  
Dr. M. Y. Seh**

**Submitted in Partial Fulfillment of the Requirements for the  
Degree of Master of Science in Physics, Faculty of Graduate  
Studies, at An-Najah National University at Nablus,  
Palestine .**

**May,2001**



*An-Najah  
National University*

*Faculty of Graduate Studies  
Physics Department*

# **THE MAGNETIC PROPERTIES OF THE ALLOYS Fe(Al,Mn) SYSTEM**

**BY  
Sabri Ahmed Al-Tannah**

**Supervisor  
Dr. M. Y. Seh**

**Submitted in Partial Fulfillment of the Requirements for the  
Degree of Master of Science in Physics, Faculty of Graduate  
Studies, at An-Najah National University at Nablus,  
Palestine .**

**May,2001**

11

# **THE MAGNETIC PROPERTIES** **OF THE ALLOYS Fe(Al,Mn)** **SYSTEM**

**BY**  
**Sabri Ahmed Al-Tannah**

**This Thesis was defended successfully on 18- June -2001 and approved by**

**Committee Members**

**Signature**

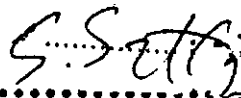
**Dr. M. Y. Seh**

.....

**Dr. M. Abu Samrah**

.....

**Dr. G. Saffarini**

.....

**Dr. S. M. Al-Jaber**

.....

**May,2001**



إهداء

أهدي عملي هذا الى نزوجتي العزيزة وأولادي الأحباء الذين وقفوا معي

وشجعوني وقدموا لي كل العون وحرصوا على مراحتي أثناء دراستي .

أتقدم منهم جميعاً بالحب والتقدير والاحترام .

## **Contents**

<i>Acknowledgments</i>	<i>VI</i>
<i>Abstract</i>	<i>VII</i>
<i>Arabic Abstract</i>	<i>IX</i>
<i>Chapter One : Introduction</i>	<i>1</i>
1-1 Previous Studies	1
1-2 Present Work	11
<i>Chapter Two: Theoretical Background</i>	<i>14</i>
2-1 Introduction	14
2-2 Alternating Current(AC) Susceptibility	16
2-3 Diamagnetism	20
2-4 Paramagnetic Susceptibility	21
2-4-1 Experiment Behavior of Transition Series Salts	26
2-5 Ferromagnetism	30
2-5-1 Curie Point and the Exchange Integral	33
2-6 Antiferromagnetism	36

<b><i>Chapter Three: Experimental Techniques</i></b>	<b>42</b>
<b>3-1 Sample Preparation</b>	<b>42</b>
<b>3-2 Experimental Devices</b>	<b>43</b>
<b>3-2-1 Water Jacket Sensor MS2W</b>	<b>44</b>
<b>3-2-2 Furnace Type MS2WF</b>	<b>47</b>
<b>3-2-3 Power Supply/Temperature Controller                 Type MS2WFP</b>	<b>49</b>
<b>3-2-4 Magnetic Susceptibility meter Tyre MS2</b>	<b>51</b>
<b>3-2-5 Personal Computer</b>	<b>55</b>
<b>3-3 Susceptibility Measurement</b>	<b>55</b>
<b><i>Chapter Four: Results and Discussions</i></b>	<b>60</b>
<b>4-1 Results</b>	<b>60</b>
<b>4-2 Discussion</b>	<b>62</b>
<b>4-3 Summary and Conclusion</b>	<b>68</b>
<b><i>References</i></b>	<b>84</b>

### *Acknowledgments*

First of all I would like to express my high appreciation to Prof. I. Abu-Aljarayesh for his guidance and providing the samples for this work . Also, I would like to thank Dr. M. Y. Seh for his assistance and supervising my experimental work. Also, I am grateful to Dr. M. Abu-Samrah, Dr. G. Saffarini and Dr. S. Al-Jaber for their serving as committee members .

I wish also to thank physics department at An-Najah National University especially Dr. M. El-Hassan for his fruitful help .

Finally, I would like to thank my son Nabeel for his help in printing my thesis, and my wife for her encouragement and support.

## Abstract

In this thesis we study the magnetic properties of the alloy system  $\text{Fe}(\text{Al}_{1-x}\text{Mn}_x)$ , for  $x=0.31$  ,  $0.35$  ,  $0.60$  and  $0.80$  , by measuring the susceptibility in the temperature range  $300 \leq T \leq 650 \text{ K}^\circ$  in very small ac magnetic field.

The analysis of the susceptibility curves show that the sample with  $x=0.31$  is paramagnetic, while the samples with  $x=0.35$ ,  $0.60$  and  $0.80$  are ferromagnetically ordered. The susceptibility for  $x=0.31$  obeys the Curie-Weiss law with a negative paramagnetic temperature ( $\theta_p = -144\text{K}$ ) and shows nearly a straight line with nearly the same susceptibility during all the process. For the other samples (with  $x=0.35$  ,  $0.60$  and  $0.80$ ) show the coexistence of ferromagnetic and antiferromagnetic behavior with Neel temperature ( $T_N$ )=  $335$ ,  $387$  and  $393 \text{ K}$  and with paramagnetic temperature  $\theta_p = 340, 393$  and  $425 \text{ K}$  respectively .



**It is clear that the sample with  $x=0.31$  exhibits only one paramagnetic phase, but for the other samples, two phases exist; antiferromagnetic phase below Neel temperature and paramagnetic phase above Neel temperature .**

**The  $\text{Fe}(\text{Al}_{1-x}\text{Mn}_x)$  alloy system is very sensitive to temperature and the measured values for both susceptibility and Neel temperature during heating do not coincide with those values during cooling .**

## الملخص

لقد تم في هذه الأطروحة دراسة الخصائص المغناطيسية لنظام السبيكة  $\text{Fe}(\text{Al}_{1-x}\text{Mn}_x)$  وكانت لقيم  $x : 0.60, 0.80, 0.31, 0.35$  وذلك بقياس كل من القابلية المغناطيسية ( $\chi$ ) في مدى درجات الحرارة  $300 \leq T \leq 650$  ب مجال مغناطيسي صغير جدا وب الاعتماد على جهاز قياس يعمل على مبدأ تغير التردد عند وجود العينة . ولقد أظهر تحليل البيانات أن العينة  $x=0.31$  هي مادة بارامغناطيسية وتخضع لقانون Curie-Weiss ولها  $(\theta_p)$  تساوي  $k -144$  ، وأظهرت قيمة ثابتة للقابلية المغناطيسية ( $\chi$ ) طيلة عملية التسخين . بينما العينات الأخرى ، والتي لها  $x = 0.35, 0.60, 0.80$  هي مواد فيها كل من الخاصيتين الفيرومغناطيسي والضد فيرومغناطيسي ، ولها (Neel  $T_N = 335, 387, 393 \text{ k (Temp.}$  على الترتيب . وتبين من التحليل أيضا أن  $(\theta_p)$  هي على التوالي  $340, 393, 425$  .

أن هذا النظام السبيكي حساس جدا عند معاملته بالحرارة . وقد أظهرت النتائج أن قيم القابلية المغناطيسية ودرجة حرارة نيل (Neel) أثناء التسخين تختلف عن نظيراتها أثناء التبريد .

# ***Chapter One***

## **Introduction**

### ***1-1 Previous studies***

**Intermetallic compounds containing one or more of the iron group continue to provide an arena for enormous advances in understanding the behavior and the applications of many aspects of magnetism . This was motivated for the need of a better understanding of the structural and magnetic properties of these compounds .**

**The equiatomic intermetallic compounds FeAl ,having the ordered B2 CsCl- type structure with a lattice constant  $a \approx 2.89\text{\AA}$  is paramagnetic, (Fig 1-1)[1].**

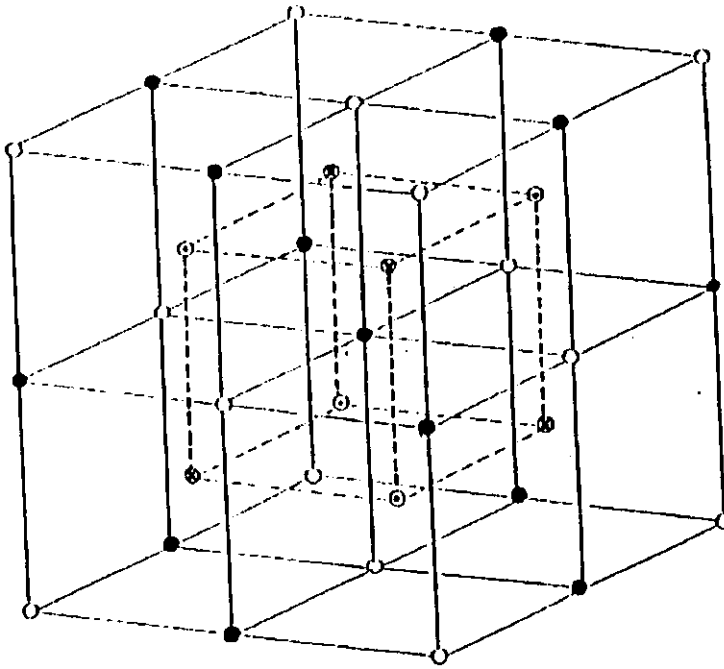


**Fig.(1-1). Unit cell of four interpenetrating FCC sublattices showing the four types of site at  $A(0,0,0)$  (o),  $B(\frac{1}{4}, \frac{1}{4}, \frac{1}{4})$  (o),  $C(\frac{1}{2}, \frac{1}{2}, \frac{1}{2})$  (●) and  $D(\frac{3}{4}, \frac{3}{4}, \frac{3}{4})$  (⊕). Structures: B2,  $A=C$  and  $B=D$ ;  $L2_1$ ,  $A=C$  and  $B \neq D$  Ref.[1].**

In common with many of the other B2 systems described, the paramagnetic equiatomic alloy can be induced to become ferromagnetic by the substitution of other 3d elements for Al[20].

547644

The substitution of Al atoms by other transition metals T solutes with  $T=\text{Ti}, \text{V}, \text{Cr}, \text{Co}, \text{Cu}$  and  $\text{Mn}$ , results in a rich variety of structural and magnetic behavior.

The  $\text{Fe Al}_{1-x}\text{T}_x$  alloy systems with ( $T=\text{Ti}$  and  $\text{V}$ )  $0.10 \leq x \leq 0.65$  have been studied structurally and magnetically [2,13]. X-ray and neutron diffraction data for Ti and V substitutions reveal that, except for the high concentration Ti substitution ( $x \geq 0.35$ ), all the studied intermetallic compounds are single phase.

The single phase Ti and V alloys are paramagnetic, but alloys Ti with  $x \geq 0.35$  contain a second-phase, and show a spontaneous magnetization [2]).

The partially substitutions of Al by Cr solutes forming  $\text{FeAl}_{1-x}\text{Cr}_x$  with  $0.1 \leq x \leq 0.5$  have been also studied structurally and magnetically [2].

X-ray and neutron diffraction measurements show that the system remains B2-type structure in the composition range studies. It was found that Cr atoms enter the Fe sites preferentially, with a consequent displacement of atoms to Al site, which becomes noticeable beyond  $x=0.20$ , this is known as B2<sub>1</sub> model type structure (Fig.1-1). Ferromagnetism was observed in the Cr system for  $x=0.35$ .

The structural and magnetic properties of the Fe Al<sub>1-x</sub> Co<sub>x</sub> system with  $0.05 \leq x \leq 0.45$ , have been investigated by various experimental techniques [3,12,20].

The results of X-ray diffraction and scattering have indicated that the alloy series exhibited a B2<sub>1</sub> CsCl-type structure with a lattice constant  $a \approx 2.91 \text{ \AA}$ . Which decreases linearly with increasing Co-concentration [5]. The A-sites are randomly occupied

by Fe and Co atoms while B-sites are randomly occupied by Fe and Al atoms as is concluded from both small angle neutron scattering and Mossbauer studies [4]. The displacement of Fe atoms into Al sites creates an “antistructure” (AS) Fe atoms. Moreover, magnetization and Mossbauer spectroscopy studies have shown that the alloys with  $x > 0.35$  ordered ferromagnetically with  $T_c > 700\text{K}$ , and the alloys with  $x < 0.20$  are paramagnetic down to  $4\text{K}$ . The alloys with  $x = 0.25$ , and  $0.3$  are superparamagnetic [4,12]. It is worthwhile to mention that Ko and Yoon [11] have shown that the magnetic properties of  $\text{Fe}(\text{Al},\text{Co})$  system are sensitive to heat treatment of the sample. In fact, they found that in general the rapidly solidified (RS) samples show stronger behavior than the corresponding annealed samples. A magnetically

ordered behavior was observed for  $x \geq 0.35$ . with an estimated Curie temperature ( $T_c$ )  $\approx 380$  K [4] .

The  $\text{Fe Al}_{1-x}\text{Cu}_x$  ( $0.05 \leq x \leq 0.40$ ) alloy systems have been studied by different groups [7-10]. The results of X-ray and neutron diffraction measurements reveal that the system exhibits a B2 CsCl-type structure with a constant lattice parameter  $a \sim 2.91 \text{ \AA}$  for  $x \leq 0.40$ . The Cu atoms are equally distributed among the Fe and Al sites, thus forming a  $\text{B2}_3$  –model type structure (Fig. 1-1) .

It was found that ferromagnetism properties appeared in these alloys with  $x \geq 0.30$  , while the alloys with  $x \leq 0.25$  remains paramagnetic down to 77K. In the ferromagnetic region the magnetization increases as  $x$  increases and so does the Curie temperature. Kim and Yoon[8] have shown that the magnetic properties of  $\text{Fe(Al,Cu)}$  system are sensitive to heat treatment,



they found that the RS samples show a higher magnetization and Curie temperature than those of the annealed ones, which is similar to the behavior of Fe(Al,Co) system . The RS alloys, however, exhibited some extent of disorder in the site occupancies of Al atoms and Fe atoms[8]

The  $\text{FeAl}_{1-x}\text{Mn}_x$  system which is the subject of the present work has also been studied structurally and magnetically by different workers [4,13] up to  $x \sim 0.40$ . X-ray and neutron diffraction measurements are consistent with B2-type structure, representing a model for which the Mn atoms exercise a site preference for the Al sites to the Fe sites in the ratio of 3:2 [4]. This distribution necessitates the displacement of Fe atoms to Al sites and consequently creates Fe Al atoms [4], (Fig.1-1). An apparent onset of spontaneous magnetization was observed beyond the critical

concentration  $\sim 0.30$ . Although no Curie temperature could be obtained from Arrott plots for the Mn series having  $x=0.40$ . Mossbauer studies on the same sample used in reference [4] did not show any ferromagnetic behavior at room temperature [13].

At this point, we will present a summary of site occupation by various constituent atoms for different systems. Also from previous discussions of  $\text{Fe Al}_{1-x}\text{T}_x$  systems we will present a summary of the critical concentration  $x_{\text{crit}}$  for transition from one structure order to another  $x_{\text{crit}}$  for onset of spontaneous magnetization in Tables (1-1) and (1-2) respectively.

Structure	Site A	Site B	Site C	Site D
B2 <sub>1</sub>	Fe	Al <sub>1-x</sub> T <sub>x</sub>	Fe	Al <sub>1-x</sub> T <sub>x</sub>
B2 <sub>2</sub>	Fe <sub>1-x</sub> T <sub>x</sub>	Al <sub>1-x</sub> Fe <sub>x</sub>	Fe <sub>1-x</sub> Tx	Al <sub>1-x</sub> Fe <sub>x</sub>
B2 <sub>3</sub>	Fe <sub>1-y</sub> T <sub>y</sub>	Al <sub>1-x</sub> T <sub>x-y</sub> Fe <sub>y</sub>	Fe <sub>1-y</sub> T <sub>y</sub>	Al <sub>1-x</sub> T <sub>x-y</sub> Fe <sub>y</sub>
L2 <sub>1(i)</sub>	Fe	Al	Fe	Al <sub>1-2x</sub> T2 <sub>x</sub>
L2 <sub>1(ii)</sub>	Fe <sub>1-2x</sub> T <sub>2x</sub>	Al <sub>1-x</sub> Fe <sub>x</sub>	Fe	Al <sub>1-2x</sub> Fe <sub>x</sub>
L2 <sub>1(iii)</sub> (y>x)	Fe	Al <sub>1-y</sub> T <sub>y</sub>	Fe	Al <sub>1-2x+y</sub> T <sub>2x-y</sub>

Table (1-1). The atomic distribution for various types of FeAl<sub>1-x</sub>T<sub>x</sub> structure, Ref. [2] .

Solute T	X <sub>crit</sub> for B2→L2 <sub>1</sub> ordering	X <sub>crit</sub> for magnetic ordering
Ti	0.2	-
V	0.3	-
Cr	B2→B2 <sub>2</sub> →B2 <sub>3</sub>	0.35
Mn	0.4	0.3
Fe	-	-
Co	B2→B2 <sub>2</sub>	0.3
Cu	B2→B2 <sub>3</sub>	0.3

Table (1-2). A comparison of the composition at which B2 to B2<sub>1</sub> ordering occurs (if at all) for the Fe(Al/T), and critical composition at which it is possible to infer a transition from paramagnetism to ferromagnetism is given, Refs.[4,8,11]

Also the magnetic properties of  $\text{Fe Al}_{1-x} \text{Mn}_x$  alloys have been studied with  $x=0.27, 0.29, 0.31, 0.35, 0.50$  &  $0.60$  in the temperature range  $85 \leq T \leq 300\text{K}$  and in fields up to  $8 \text{ kOe}$  [14]. In this study the magnetization increases with increasing Mn. The isothermal magnetization curves ( $M$  Vs.  $H$ ) for samples  $x=0.27, 0.29$  &  $0.31$  show straight lines which indicates an ideal paramagnetic behavior.

### ***1-2 Present Work***

In the present work ,we have studied the magnetic susceptibility of  $\text{FeAl}_{1-x} \text{Mn}_x$  with  $x=0.31, 0.35, 0.60$  and  $0.80$  in the temperature range  $300 \leq T \leq 650 \text{ K}$  in a very small alternating ac fields.

For a better understanding of the magnetic behavior of this system, the Mn-concentration is extended to a higher value ( $x=0.80$ ) and also the temperature range to a higher value ( $T \leq 650\text{K}$ ). Our initial temperature ( $T \approx 300\text{K}$ )

was a final temperature for the previous study. This gives an insight into the behavior of such systems in this temperature range and concentration . For example , the phase transition from one type of magnetic property to another .

While previous studies used heating only in recording the magnetization, the present work deals with heating the samples as well as cooling in recording the susceptibility. Also in previous studies a magnetic field was applied for different temperatures, but our study was carried out without magnetic field.

This thesis is organized as follows: Chapter two, for the relevant theoretical background , chapter three presents the experimental techniques that is used for

**carrying out this study. Chapter four presents the obtained results, discussions and finally the summary and the conclusion of this study .**

## *Chapter Two*

### **Theoretical Background**

#### *2-1 Introduction*

Measurements of the temperature dependence of the magnetic susceptibility belong to important sources of information about metal complex. After an appropriate fit of experimental data to a theoretical model, the set of magnetic parameters which characterizes the microscopic properties of the metal-containing entities (complexes, dimmers, clusters, ordered system chains ,etc) is obtained. This allows a reconstruction of the spacing of energy levels whose separation is only a few wavenumbers.

The magnetic susceptibility is introduced as a partial derivative of the magnetization with respect to the



magnetic field. Often it is assumed that the metal complexes belonging to molecular paramagnets behave like linear magnetization and thus the magnetic susceptibility could be treated as a simple ratio of the magnetization and the applied field.

$\chi = dM/dH$  , this is the differential volume magnetic susceptibility .

The mass susceptibility and molar susceptibility are respectively

$\chi_p = \chi / \rho$  where  $\rho$  is the density

$\chi_{mol} = \chi_p M_s / \rho$  where  $M_s$  is the molar mass .

In this chapter, we will present a brief theoretical treatment of ac susceptibility ,diamagnetism, paramagnetism, ferromagnetism and antiferromagnetism.

## 2-2 Alternating current (AC) susceptibility

The AC is used to generate the alternating field

Fig.(2-1)[15] . The time evolution of the magnetic field strength is given by

$$H_{AC} = H_0 \cos(\omega t)$$

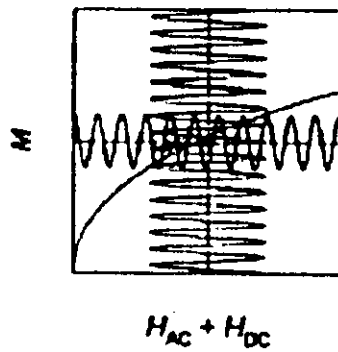


**Fig.(2-1). AC Measurement in conjunction with an applied DC field.**

where  $H_0$  is the amplitude of the applied field ,  $\omega$  is the angular frequency of the AC field ( $\omega = 2\pi\nu$  ). The magnetization  $M_{AC}$  [15] cannot follow the incident

field immediately and it is shifted by a phase angle  $\theta$  ,  
so that

$$M_{AC} = M_0 \cos (\omega t - \theta) \quad (2-1)$$

This formula can be rewritten as

$$M_{AC} = \chi' H_0 \cos(\omega t) + \chi'' H_0 \sin(\omega t) \quad (2-2)$$

with  $\chi' = (M_0 / H_0) \cos \theta \quad (2-3)$

$$\chi'' = (M_0 / H_0) \sin \theta \quad (2-4)$$

The quantity just introduced is the magnetic susceptibility having two components . The in-phase (real) component is  $\chi'$  and it corresponds to the dispersive magnetic response . The out-of-phase (imaginary) component is  $\chi''$  and it corresponds to the energy dissipation (that is the energy absorbed by the material from the applied AC field : it is termed the absorption) . Normally  $\chi''$  is very small positive

quantity. The AC susceptibility, can be viewed as a complex quantity

$$\chi = \chi' + i\chi'' \quad (2-5)$$

The components of the AC susceptibility depend upon the frequency of the applied field. When the frequency is low, the magnetization can readily follow the applied field so that the low-frequency limit corresponds to the isothermal susceptibility

$$\lim_{\omega \rightarrow 0} \chi = (\partial M_{AC} / \partial H)_T = \chi_T \quad (2-6)$$

This is comparable with the susceptibility measured in static fields. The greater the frequency, the lower the AC susceptibility, which in the opposite limit approaches the adiabatic value

$$\lim_{\omega \rightarrow \infty} \chi = (\partial M_{AC} / \partial H)_S = \chi_S \quad (2-7)$$

The recovery of a perturbed system to a new equilibrium is described by introducing the relaxation time

$$dM/dt = (M(\infty) - M(t)) / \tau \quad (2-8)$$

where  $M(\infty)$  is the equilibrium magnetization and  $M(t)$  is the magnetization at time  $t$ .

The isothermal , adiabatic and AC susceptibilities are interrelated through Fig. (2-2) [15].

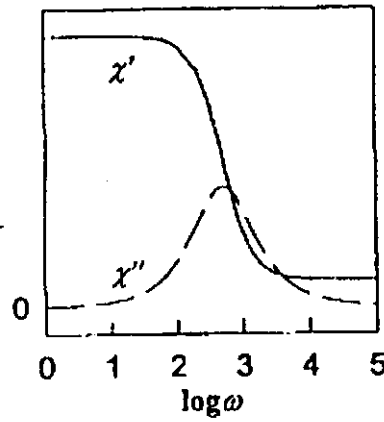


**Fig.(2-2). Frequency dependence of the AC susceptibility .**

The alternating magnetic field can be combined with an admixture of the constant field generated by a direct current (DC) . The magnetic moment is induced in a sample through the application of the DC

bias field , produced either by the primary coil or by a superconducting magnet .

### ***2-3 Diamagnetism***

Diamagnetic substances have a negative susceptibility. All substances have a basic diamagnetic but it is nearly always weak and it is very often masked by a much larger (positive) paramagnetic susceptibility . The basic independent of temperature is due to the applied magnetic fields which affects the motion of inner electrons of the atoms present . The electronic orbits around the nuclei of atoms were considered as though they are magnetic moments of electric currents . When a magnetic field is applied the electron motion is modified and the magnetic moment due to the currents is changed [16]. Lenz's law of electromagnetic induction states that currents induced by a magnetic field are in such a direction that their magnetic fields tends to oppose the

change of the original inducing field. That is, the induced magnetization is negative and so is the susceptibility . Mostly , this is one or two orders of magnitude weaker than typical paramagnetic susceptibility and is only observed as a relatively minor correction which is usually independent of temperature .

#### ***2-4 Paramagnetic Susceptibility:***

Many solids are paramagnetic. When a field is applied to them they become magnetized. Usually, paramagnetic materials are much more weakly than ferromagnetic materials .

Paramagnetic materials exhibit a small magnetic susceptibility in the presence of a magnetic field . Paramagnetism produces magnetic susceptibilities in the order of  $10^{-6}$ . Table (2-2) lists magnetic susceptibilities of paramagnetic and diamagnetic at 20°C. Paramagnetism is produced by the alignment

of individual magnetic dipole moments of atoms and molecules in an applied magnetic field . The atoms of some transition elements posses incompletely filled inner shells with unpaired electrons . The unpaired inner electrons in atoms, since they are not counterbalanced by other bonding in solids cause strong paramagnetic effects [6] .

Diamagnetic element	Magnetic susceptibility $\chi_m \times 10^{-6}$	Paramagnetic element	Magnetic susceptibility $\chi_m \times 10^{-6}$
Cadmium	-0.18	Aluminum	+0.65
Copper	-0.086	Calcium	+1.10
Silver	-0.20	Oxygen	+106.2
Tin	-0.25	Platinum	+1.10
Zinc	-0.157	Titanium	+1.25

**Table (2-2). Magnetic susceptibilities of some diamagnetic and paramagnetic elements , Ref. [6] .**



The rate of change of the magnetization with field is called the paramagnetic susceptibility, which is referred to the unit mass of the specimen ( $\chi$ ), to one mole ( $\chi_m$ ) or to a unit volume ( $\kappa$ ).

Above the Curie temperature ferromagnetic materials become paramagnetic ones and their susceptibility depends on temperature. The reciprocal of the susceptibility varies linearly with temperature, or nearly so (Fig. 2-3), whose intercept on the positive temperature axis is the paramagnetic Curie temperature  $\theta_p$ .  $\theta_p$  is usually of the same order as  $T_c$  but the two quantities are rarely exactly equal. The dependence of susceptibility on temperature is shown in (Fig. 2-3). This type of dependence is known as the Curie-Weiss law.

$$\chi = C/(T - \theta_p) \quad (2-9)$$

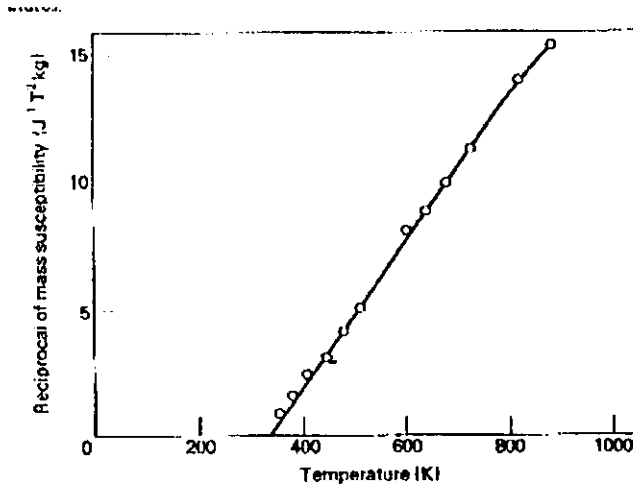


**Fig.(2-3). The reciprocal of susceptibility plotted against temperature for nickel-32% copper alloy illustrating the curie-Weiss law .  $\theta_P$  is 336k**

For some compounds such as hydrated copper sulphate  $\theta_P$  is zero, and then Curie law, becomes  $\chi = C/T$  . Negative values of  $\theta_P$  are also found, in antiferromagnetics above their Neel temperature ( $T_N$ ). The constant  $C$  and  $\theta_P$  are attributed to the fundamental properties of the atom or ions of the materials .

Many non-ferromagnetic metals are paramagnetic but their susceptibility is relatively weak and has a very weak dependence on temperature (Fig. 2-4). In such materials paramagnetism is generally a property of electrons contained in a relatively broad energy bands associated with the metallic state [16].

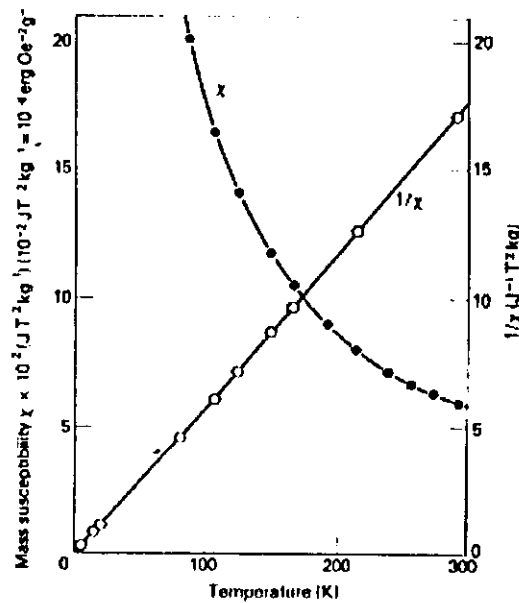


**Fig.(2-4). The susceptibility and its reciprocal plotted against temperature for  $\text{CuSO}_4 \cdot 5\text{H}_2\text{O}$  (Curie law).**

### ***2-4-1 Experimental Behavior of Transition Series Salts .***

The experimental susceptibilities of transition metals do not support the free ion theory at all. This is because the d-electrons are involved in a varying the crystal bonding degree and conduction. The free ion model is not applicable. Salts in the first transition series of elements, the agreement with the simple free ion theory is also limited. However, if it is assumed that the orbital moment plays no part in the magnetism and that the moment is totally for spin, the experimental and, the calculated values of the effective paramagnetic Bohr magneton number ( $P_{eff}$ ) agree quite well for many of such salts (Fig. 2-5)[16].

The value of  $P_{eff}$  then becomes  $P_{eff} = 2[S(S+1)]^{1/2}$  ,  
since when  $L=0$  ,  $g$  has the value 2

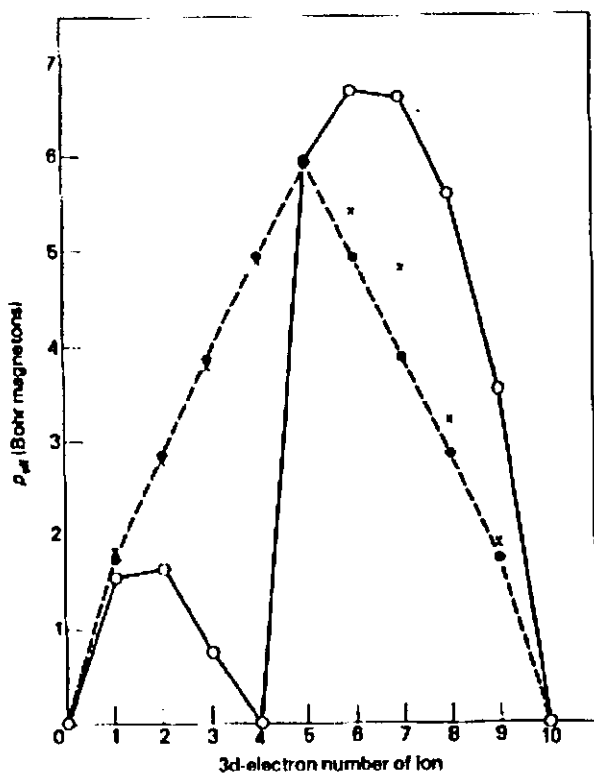


**Fig.(2-5).** *The experimental and the calculated values of  $P_{eff}$  for ions of the first transition series . x: experiment; O and full line , calculated for full J; • and broken line, calculated for spin only .*

The reason for the loss of orbital moment is because of the magnetic electrons in transition series ions are not screened by significant distributions of charge . The partially filled 3d-shells feel the effect of

anisotropic crystalline electric fields produced by their environment. In the first transition series the effect of crystal field is stronger than those of spin-orbit coupling, but not so strong as to set up the resultant vectors  $S$  and  $L$ . This contrasts with the behavior of rare-earth ions, where the spin-orbit coupling is stronger than the crystal field effect [16] .

consequently, for transition metal ions from the iron group, one finds that, the value of Bohr magneton number ( $P$ ) determined by the following relation [17]

$$P = g(J L S) [J (J+1)]^{1/2} \quad (2-10)$$

and Curie's law is fulfilled as well as Hund's rule. This phenomenon is known as the quenching effect of the orbital angular momentum. This is a particular example of a general phenomenon known as a crystal field splitting.

Crystal field splitting is important for the partially filled d-shells of transition metal ions, which are strongly influenced by their crystalline environment. Fig.(2-6)[19] illustrates both the magnetic susceptibilities for diamagnetic and paramagnetic materials including negative and positive susceptibilities respectively.

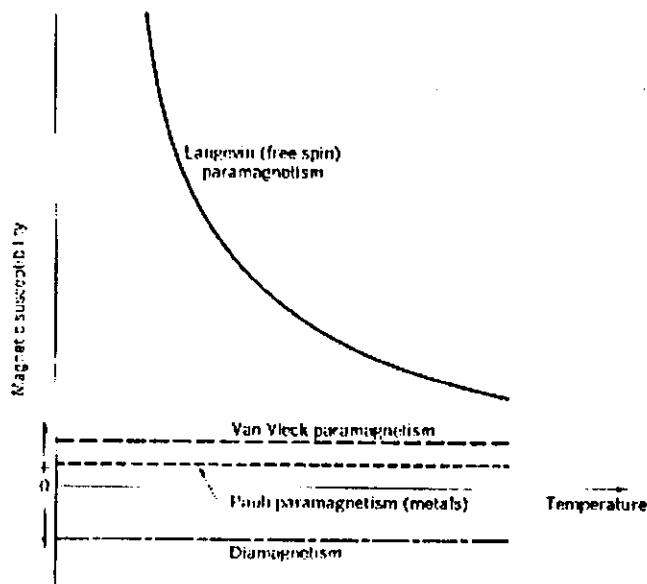


**Fig.(2-6). Illustration of the characteristic magnetic susceptibilities for both diamagnetic and paramagnetic substances.**

## ***2-5 Ferromagnetism***

**In ferromagnetic materials the dipoles alignment represents an increase in the degree of order within the solid, and thus a decrease in entropy . In the magnetic order of ferromagnetism , all moments contribute equally to the spontaneous magnetization . The most widely recognized magnetic elements are iron , nickel and cobalt. The measured magnetization depends on the dipole moment of the specimen and the induction within the specimen is measured from the charge flowing in a closed electrical circuit when the specimen is inserted in or removed from it. The magnetization is used for calculating the ferromagnetic properties, while the induction is used for technical purposes. The magnetization for ferromagnetic materials does not return to zero when the field is switched off and it**



remains at a value only a little below its value in a strong field, this which is called the spontaneous magnetization.

The spontaneous magnetization depends on temperature, and attains its maximum value at the absolute zero. It falls rapidly with increasing temperature and becomes zero at a temperature called Curie temperature,  $T_c$ . The maximum value of the spontaneous magnetization at  $T=0$  is directly related to the average magnetic moment per atom of the ferromagnetic and it is a measure of the number of magnetic carriers per atom [16].

In a zero magnetic field and with a density of atoms  $Nm^{-3}$ , the magnetization is

$$\begin{aligned}\bar{M} &= N \mu = (Ng \beta J B_J(x)) / 3KT \\ &= (Ng^2 \beta^2 J(J+1) B_0) / 3KT\end{aligned}\quad (2-11)$$

and the zero field susceptibility is

$$\chi = M/H_0 = M/(B_0/\mu_0)$$

$$\text{i.e } \chi = (\mu_0 N g^2 \beta^2 J(J+1)) / 3KT \quad (2-12)$$

which is the general form of the Curie law ,  $\chi = C/T$ .

For one electron per atom in an S-state with  $L=l=0$

and thus  $J = S$  and  $s = \frac{1}{2}$  , we have

$$\chi = \mu_0 N g^2 \beta^2 (3/4) / 3KT = \mu_0 N g^2 \beta^2 / (4KT) .$$

The levels and magnetic moments for  $J=1$  are shown in (Fig.2-7)[18].

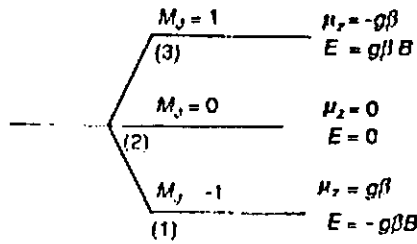


**Fig.(2-7). Energy level splitting for coupled states due to a magnetic field,  $J=1$  .**

### ***2-5-1 Curie Point and the Exchange Integral .***

Consider a paramagnet with a concentration of  $N$  ions of spin  $S$ . Given an internal interaction of tending to line up the magnetic moments parallel to each other, we have a ferromagnet. Let us assume such an interaction and call it the exchange field or molecular field or the Weiss field ( $B_E$ ). The orientation effects of the exchange field are opposed by thermal agitation, and at high temperatures the spin order is destroyed, then the exchange field is treated as equivalent to a magnetic field. If domains (regions magnetized in different directions) are present the magnetization refers to the value within a domain. In the mean field approximation we assume each magnetic atom experiences a field proportional to the magnetization.

$$B_E = \lambda M \quad (2-13)$$

Where  $\lambda$  is a constant independent of temperature. Each spin sees the average magnetization of all other spins. For  $T > T_c$ , the spontaneous magnetization vanishes and separates the disordered paramagnetic phase ( $T > T_c$ ) from the ordered ferromagnetic phase ( $T < T_c$ ). one can find  $T_c$  in terms of  $\lambda$ .

Consider the paramagnetic phase in which an applied field  $B_a$  causes a finite magnetization and in turn, causes a finite exchange field  $B_E$ . If  $\chi_p$  is the paramagnetic susceptibility, the magnetization can be written as

$$M = \chi_p (B_a + B_E) \quad (\text{CGS}) \quad (2-14)$$

If Curie's law is applicable,  $\chi_p = C/T$ , then  $MT = C(B_a + \lambda M)$  and

$$\chi = M/B_a = C/(T - C\lambda) \quad (2-15)$$

Clearly, the susceptibility has a singularity at  $T = C\lambda$ . At this temperature and below there exists

a spontaneous magnetization, because  $\chi$  has infinite value for a finite  $M$  in the absence of  $B_a$ . From eqn. (2-15), the Curie Weiss law becomes

$$\chi = C / (T - T_c) \quad , \quad T_c = C \lambda \quad (2-16)$$

This expression describes well the observed susceptibility variation in the paramagnetic region above the Curie point. The reciprocal susceptibility of nickel is plotted in (Fig.2-8)[19].

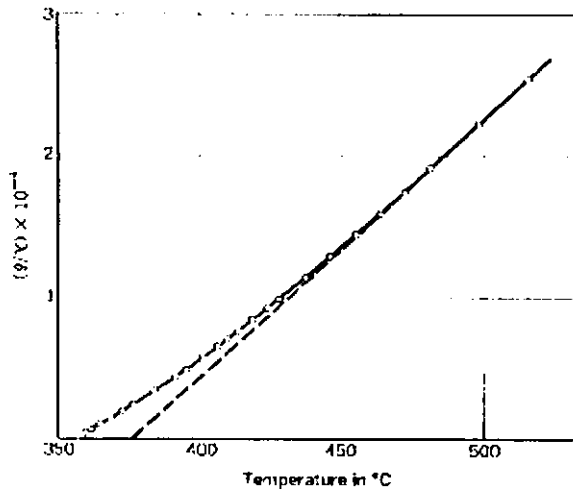


**Fig.(2-8).** The reciprocal of the susceptibility per gram of Nickel in the neighborhood of the curie temperature (358°C). The dashed line is a linear extrapolation from high temperatures. Analysis of the curve near  $T_c$  has been given by J.S. Kouvel and M.E. Fisher, *Phys. Rev.* 136,A166.(1964)

The value of the mean field constant,  $\lambda$ , is determined from eqn.(2-16) and Curies law, as

$$\lambda = T_c / C = (3K_B T_c / (N g^2 S(S+1) \mu_B^2)) \quad (2-17)$$

where for iron,  $T_c \approx 1000$  K,  $g=2$ ,  $S=1$ , and  $\lambda \approx 5000$ .

For  $M_s \approx 1700$  we have  $B_E \approx \lambda M = (5000)(1700) \approx 10^7$  G.

The exchange field in iron is very much stronger than the real magnetic field due to the other magnetic ions in the crystal, in which case a magnetic ion produces a field  $\approx \mu_B / a^3$  of about  $10^3$  G at a neighboring lattice point to the ion[19].

## 2.6 Antiferromagnetism

Antiferromagnetic materials are those whose magnetic moments ordered with zero bulk spontaneous magnetization and are sometimes difficult to recognize superficially. In its simplest situation their paramagnetic

state at relatively high temperature follows Curie-Weiss law with a negative  $\theta_p$ . There is a maximum susceptibility at Neel temperature  $T_N$ . Below this temperature material becomes antiferromagnetic. At lower temperatures, the susceptibility decreases with decreasing temperature .

This might be attributed to the fact that the remaining nonferromagnetic members of the first 3d transition series of elements (Mn,Cr,V,Ti,Sc) might have a negative interaction that led to a theoretical study of the properties of antiferromagnetic system[16]

The spin arrangements of  $Mn^{++}$  shown in Fig. (2-14) are resulted from the neutron diffraction and magnetic measurements. The spins in a single [111] plane are parallel, but in adjacent [111] planes are antiparallel. Thus, MnO is classified as an antiferromagnetic substance as in Fig.(2-9).

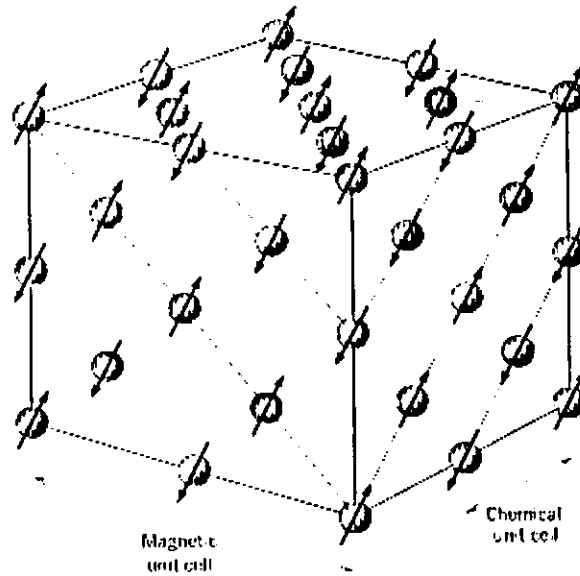


**Fig.(2-9). Ordered arrangement of spins of the  $Mn^{++}$  ions in manganese oxide . MnO as determined by neutron diffraction . The  $O^{2-}$  ions are not shown .**



**Fig.(2-10). Spin ordering in ferromagnetic ( $J > 0$ ) and antiferromagnetic ( $J < 0$ ) .**



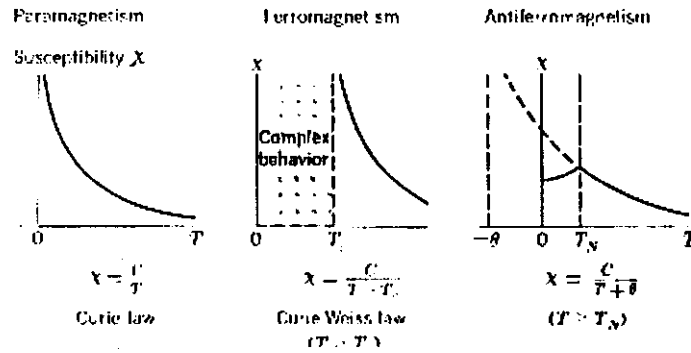


**Fig.(2-11). Temperature dependence of the magnetic susceptibility in paramagnets , ferromagnets ,and antiferromagnets. Below the Neel temperature of an antiferromagnet the spins have antiparallel orientations, and susceptibility attains its maximum value at  $T_N$  where there is well-defined knick in the curve of  $\chi$  versus  $T$ . The transition is also marked by peak in the heat capacity and the thermal expansion coefficient .**

In antiferromagnetic materials, the spins are ordered in an antiparallel arrangements with a zero net moment at temperatures below the ordering or Neel temperature . The susceptibility of antiferromagnet is not infinite at  $T= T_N$  , but has a weak cusp, as in Fig.(2-11) . The Neel temperature as defined in the mean field approximation is given by

$$T_N = \mu C \quad (2-18)$$

where  $C$  refer to single sublattice . The susceptibility in the paramagnetic region  $T > T_N$  is given by

$$\chi = (2CT - 2\mu C^2)/(T^2 - (\mu C)^2) = 2C/(T + \mu C) = 2C/(T + T_N) \quad (2-19)$$

while the experimental results at  $T > T_N$  is of the form

$$(CGS) \quad \chi = C/(T + \theta_p) \quad (2-20)$$

This is the Curie –Weiss law with, a negative paramagnetic temperature  $\theta_p$  .

The magnetization in the antiferromagnetic regions for  $T < T_N$ , where each sublattice is spontaneously magnetized , in zero applied field, by the molecular field created by the other sublattice is

$$M = M_A + M_B = 0 \quad (2-21)$$

$$\text{or} \quad M_A = -M_B \quad (2-22)$$

At any temperature below  $T_N$ , the magnetization of A sublattice will be given by the Brillouin function :-

$$M_A = M_{oA} B_J(x) \quad (2-23)$$

where  $x = g J M_B H / KT$  , and  $K$  is the Boltzman constant .

Similary the magnetization of atoms in B sublattice can be calculated [18] .

## ***Chapter Three***

### ***Experimental Techniques***

#### ***3-1 Sample Preparations***

The alloy series of  $\text{FeAl}_{1-x}\text{Mn}_x$  with  $x=0.27$  0.29 0.31 , 0.33 , 0.60 and 0.80 , were fabricated using arc furnace , melting the proper amounts of spec-pure materials in an argon atmosphere , forming a series of alloy buttons . Needle shaped samples were obtained from the buttons, which were then annealed under vacuum for 24 hours at a temperature  $830^\circ\text{C}$  and then rapidly quenched into water. The concentration of Manganese and the mass of the samples are listed in Table(3-1) .

<b>Mn concentration(x)</b>	<b>Mass (gm)</b>
<b>0.27</b>	<b>0.7432</b>
<b>0.29</b>	<b>0.7848</b>
<b>0.31</b>	<b>2.5647</b>
<b>0.33</b>	<b>1.0160</b>
<b>0.35</b>	<b>1.1258</b>
<b>0.60</b>	<b>0.8019</b>
<b>0.80</b>	<b>1.1264</b>

**Table (3-1): The mass of the  $\text{FeAl}_{1-x}\text{Mn}_x$  samples with Manganese concentration (x) .**

### ***3-2 Experimental Devices***

**All the magnetic susceptibility measurements were carried out using “MS2 Magnetic Susceptibility System” . This setup is illustrated in Fig. (3-1), and manufactured by “Bartington Instruments Company”.**

The portable MS2 system can be used to measure both low field and frequency –dependent susceptibility .

The MS2 system comprises the following :-

### ***3-2-1 Water Jacket Sensor MS2W (Fig. (3-2)) .***

The highly stable sensing coil, together with precision oscillator electronics within sensor enclosure Fig. (3-2) [21] are cooled by a flow of cold water which completely screens the sensor from extremes of temperature within the sample cavity . The special circuitry compensates for small changes in temperature arising from the influence of the furnace . The glass cavity is 65 mm high and 30 mm internal diameter and is painted on the outer surfaces with a special reflecting paint . The sensor can be mounted on a retort stand with the cavity vertically orientated when used in conjunction with the furnace. The probe is calibrated to accept a 10 cc sample. The operating frequency of 696 Hz is chosen to be

sufficiently low so that measurements are essentially independent of sample conductivity .

The specification of the Sensor type MS2W is listed below

<b>Materials</b>	<b>:Glass filled polycarbonate/glass</b>
<b>Measurement period</b>	<b>: 1.3 s on x 1.0 CGS range</b>
<b>Operating frequency</b>	<b>: 696 Hz</b>
<b>Calibration</b>	<b>:<math>\chi</math> for 10cc cylindrical sample <math>\chi/4</math> for 2.5cc (15 mm dia.) cylindrical ( furnace ) sample .</b>
<b>Calibration accuracy</b>	<b>: 1.0%</b>
<b>Measurement drift</b>	<b>: <math>&lt; 1 \times 10^{-6}</math> cgs/<math>^{\circ}</math>C of <math>1 \times 10^{-6}</math> cgs/ hour typical</b>
<b>coolant (water) flow rate</b>	<b>: 2 liters/min minimum recommended</b>

The sensor is calibrated to measure susceptibility for 10 cc cylindrical sample . The sample is put in the center of the sensor cavity.

The MS2W sensor produces a small AC field at about 696 Hz. The sensor reads magnetic susceptibility by measuring the very small change in the frequency which occurs when a sample is present in the cavity of the sensor. This can be explained by the following equation

$$f = 1/2\pi ( 1/LC )^{1/2} \quad (3-1)$$

We know that the change in capacitance gives a change in electric field, but the change in inductance gives a change in magnetic field . The induction (B) in a medium is given in eqn. (3-2)

$$B = \mu_o (H+M) = \mu_o (1+\chi_m ) \quad (3-2)$$

and

$$B = \mu H \quad (3-3)$$

$$\mu = \mu_o (1+ \chi_m) \quad (3-4)$$



Where  $\mu$  is the permeability of the sample, and  $\mu_0$  is the permeability of air . The MS2 meter reading is zero for no material inside the cavity of the sensor, which is consistent with eqn. (3-4) if we put  $\mu_0$  for  $\mu$  then the susceptibility is zero. If a magnetic material is inserted into the cavity of the sensor and we use eqn. 3 then we have a reading for susceptibility  $\chi$  . In other words we can say that inserting a material in the sensor changes the inductance and also the frequency which finally is measured by MS2 meter .

### ***3-2-2 Furnace Type MS2WF (Fig.(3-3))***

The furnace has been specially designed for use with water jacketed sensor type MS2W to facilitate susceptibility / temperature measurements up to 900 °C . The 17mm internal diameter silica tube is non-inductively wound over a 45 mm length with a platinum wire heating element which, when supplied with current, will uniformly heat a sample placed at its center. Stray

magnetic fields within the furnace are free from magnetic contaminants and contain no asbestos . The recommended sample size to obtain uniform heating is 15 mm diameter x15 mm length . The sample is placed in close contact with the tip of the type "S" built in thermocouple . In this way very accurate temperature measurements of the sample are accomplished . The sample should not come into contact with the furnace wall . Silica fibra insulating plugs are fitted at the heated section . The thermocouple linearisation circuit accepts a voltage input from either the built – in type "S" or external type "T" thermocouple . A switch is used to select the appropriate thermocouple . Specifications for this furnace are as follows :

**Materials : Silica/platinum/alumina/stainless steel**

**Electrical resistance : 3 ohms at room temperature**

**Power requirements : 100 W max. 28 V dc at 3 A**

**Internal magnetic field : measured less than 0.05 A/m**

**Operating temperature : 900°C maximum intermittent**

**Fixed thermocouple (non magnetic, high temperature )**

**Type : 'S' (Pt./Pt. 10%Rh) built-in**

**Calibrated range : 0 to 900°C**

**Separate Thermocouple (non magnetic, low temperature )**

**Type : 'T' (Cu/Cu Ni) Remote connection.**

**Calibrated range : -200°C to +150°C .**

### ***3-2-3 Power supply/ Temperature Controller Type***

***MS2WFP. (Fig,(3-4))***

**This unit performs two basic functions :**

- i) Thermostatic power control of furnace type MS2WF.**
- ii) Control of data transmissions .**

Filtered main supply is rectified and smoothed to  $\pm 25$  dc max . (20V full load) and supplied to power controlling transistors which control the voltage applied to the furnace . Furnace current is monitored by a meter on the front panel . A  $\pm 12$ V dc regulated supply is fed to the digital panel meter and associated circuitry and a precision reference voltage is provided for temperature offset and control purposes .

The furnace can be powered in one of two ways :

- (1) Per-set temperature on a 10-turn dial, thermostatically maintained .
- (2) Temperature-set programmed to increase or decrease with time in a linear fashion at rate pre-selected on the 10-turn dial .

547644

The temperature rate of change (differential) information is measured to minimize over and under

shoot which could occur when selecting a new temperature . Maximum current is limited to a 4A (cold furnace) by a self operating area monitor . The high positive temperature coefficient of resistance of the platinum furnace will limit this current to 3A maximum at elevated temperature .

#### ***3-2-4 Magnetic Susceptibility Meter Type MS2 (Fig.(3-5)).***

The portable meter display the magnetic susceptibility value of materials when these are brought within the influence of the sensor . The meter is connected to the sensor via a simple coaxial cable . An RS232 serial interface allows the meter to operate in conjunction with PC compatible software running on a portable data logger or PC . The MS2 meter is powered by internal rechargeable batteries. The circuitry within the MS2 power the sensors and processes the measurement

information produced by them . The measurements are obtained digitally using a time dependent method . This results in precise and repeatable measurement . The sensor is calibrated fully by the MS2 meter .

There are five front panel controls

**(a) Range multiplier switch**

This switch allows selection of either X 1 or X 0.1 sensitive range . In the second case the result is shown to the first place of decimal and a 10-fold increase in measurement .

Time provided additional noise filtering . The switch also activates to battery indicator .

**(b) Zero push button**

This button permits air readings to be taken . By performing a measurement to “air” this control resets the instrument and brings subsequent measurements within the range of the display .

**(C) Measure push button**

**This button permits sample readings to be taken .**

**(D) Toggle switch**

**This switch performs the same function as the push buttons , but permits continuous measurements .**

**(e) On/Off switch**

**This switch controls the internal batters supply and also permits the selection of either SI or CGS units .**

**The instrument may be pre-set to display the susceptibility value directly in one or other of the dimensional systems thus producing a basic mass or volume unit of :**

	Mass	Volume
	$\chi$	K
SI	$10^{-8} \text{ (m}^3 \text{ /kg)}$	$10^{-5}$
CGS	$10^{-6} \text{ (cm}^3 \text{ /g)}$	$10^{-6}$

The sensor must be attached to the MS2 meter for calibration . A sample mass of 10 gram is provided . For dry materials and for materials of unknown density this provides the most useful measurement because simple weighting of the material is all that required . The sample mass departs from calibration mass, then the corrected value will be :

$$\chi = \text{measured value} \times \text{calibration mass/sample mass.}$$

Therefore it will be usual to weigh carefully the samples prior to taking measurements .

Example : sample mass = 2 gram , for cal. Mass = 1gram

$$\chi_{\text{true}} = \chi_{\text{meas}}/2$$



### ***3-2-5 Personal Computer***

An RS232 connecting cable is provided with the MS2 for connection to a computer via a 25-way D-type connector. A 25 to 9-way adapter and a 9-way cable are supplied to facilitate connection to most computers. No hardware hand shaking is provided. A geolab software Dos program is used in conjunction with the susceptibility /temperature system to record the data in the selected temperature range.

The susceptibility /temperature system interconnection is illustrated in Fig.(3-6).

### ***3-3 Susceptibility Measurement***

Each sample was put in the center of the cavity of the sensor in a very small AC field. It is kept in the cavity for enough time in order to start from a stable temperature (Room temperature ~300K).

Then the temperature was increased to 650 K at the rate of 5K/min. During this , the susceptibility  $\chi$  being registered versus temperature T over the whole range  $300 \leq T \leq 650$  K , and also the same data was recorded during cooling for the samples at the same rate (5K/min.) from 650 to 300 K .

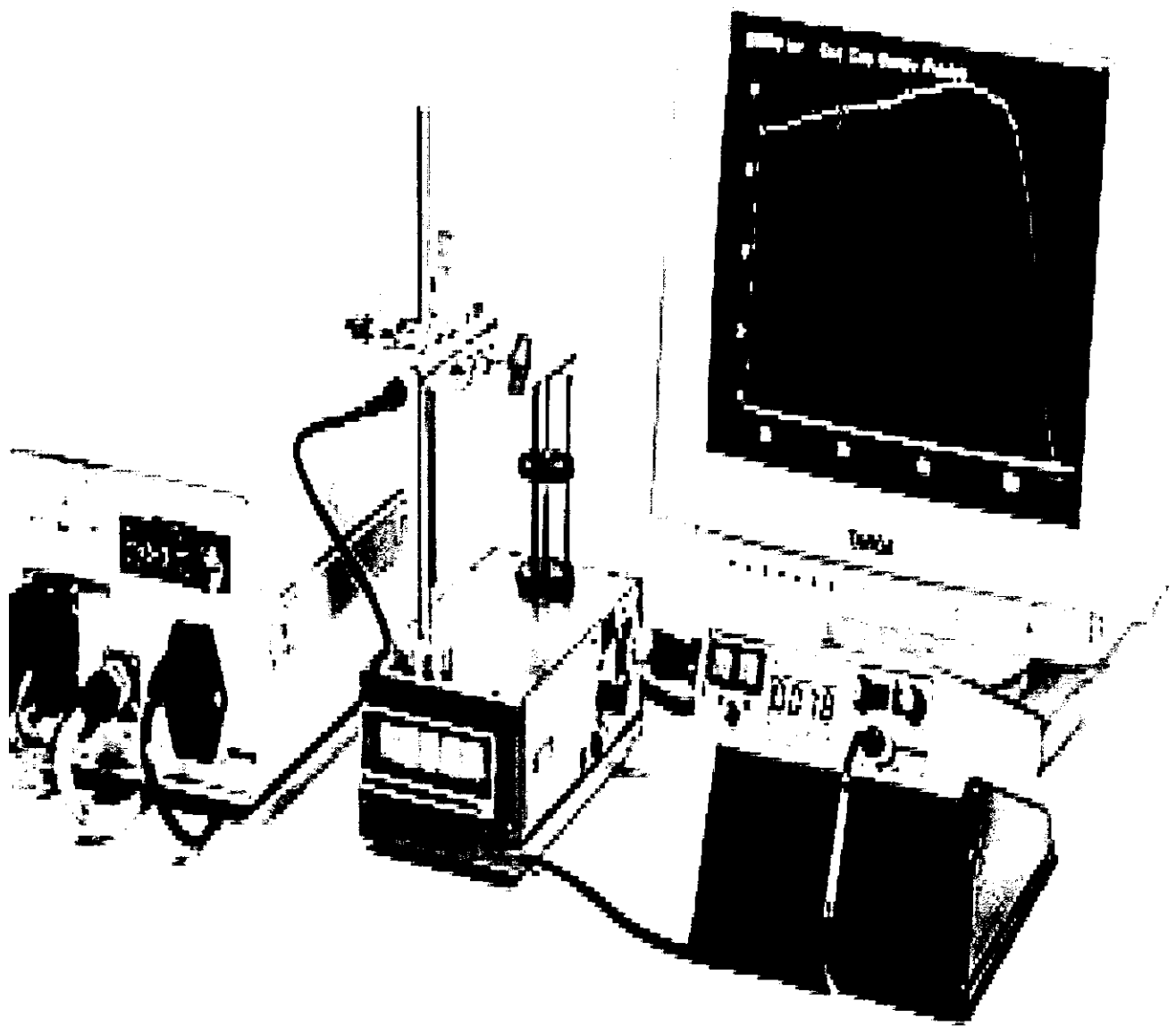


***Fig.(3-1): Magnetic Susceptibility System***

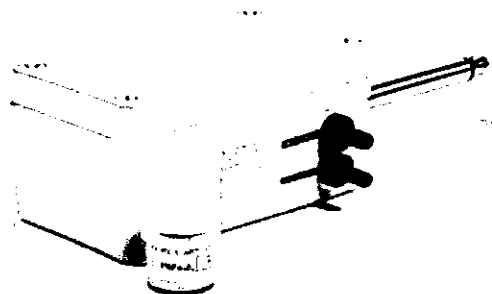


**Fig.(3-2) : Water Jacket Sensor MS2W.**

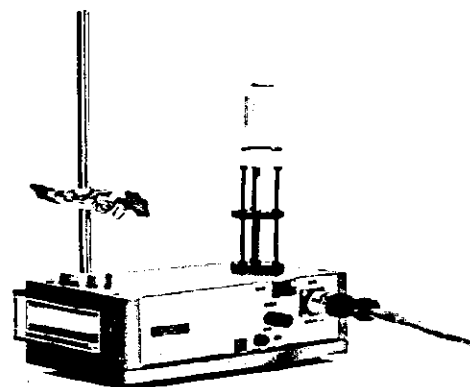


**Fig.(3-3): Furnace type MS2WF .**

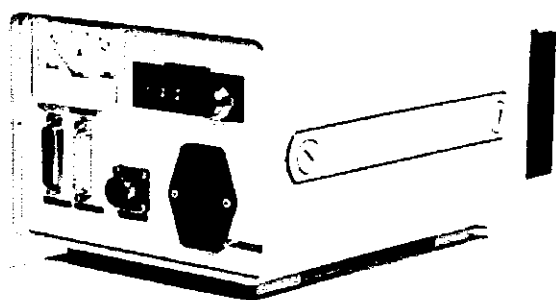


**Fig.(3-4) : Power Supply/Temperature Controller type MS2WFP .**

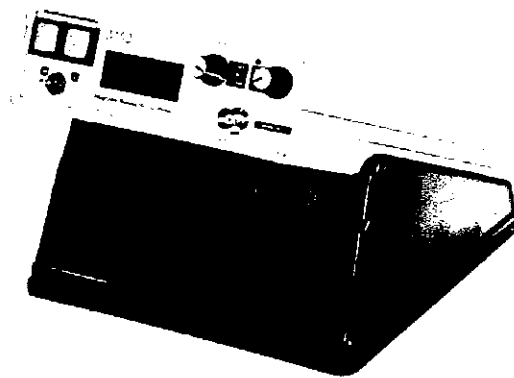
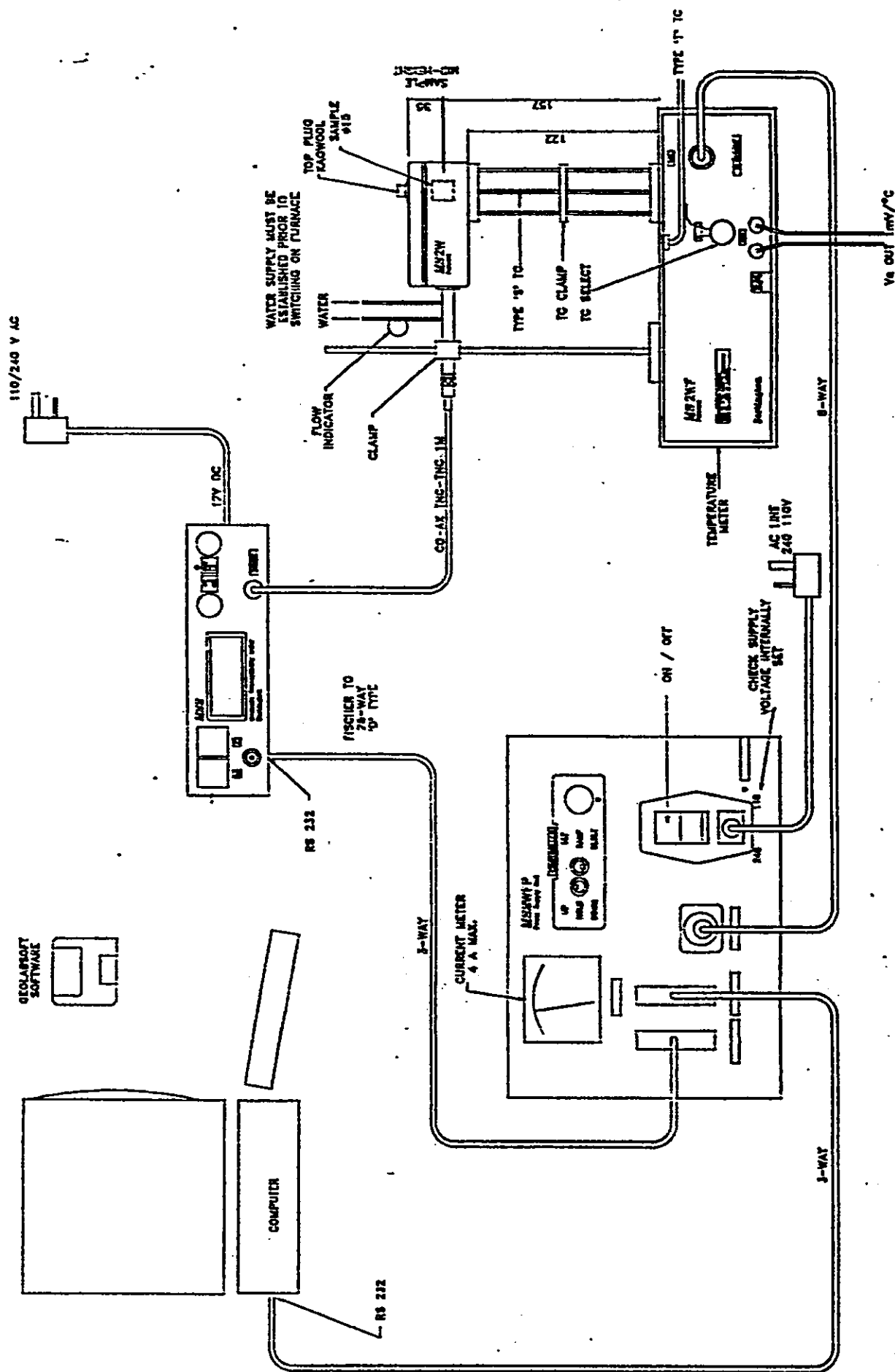


**Fig.(3-5) : Magnetic Susceptibility meter type MS2 .**



**Fig(3-6) SUSCEPTIBILITY / TEMPERATURE SYSTEM INTERCONNECTION DIAGRAM**

## ***Chapter Four***

### **Results and Discussions**

#### ***4-1 Results***

The mass susceptibility ( $\chi$ ) curves versus temperature for the  $\text{Fe}(\text{Al}_{1-x}\text{Mn}_x)$  system with  $x=0.31$  ,  $0.35$  ,  $0.60$  and  $0.80$  , are shown in figures (4-1),(4-2),(4-3) and (4-4) respectively . The susceptibility ( $\chi$ ) measured in a small AC field, depends on the change of the frequency of the sensor (696Hz) by inserting the sample into the cavity of the sensor. It is shown from the graphs that the susceptibility increases with increasing manganese concentration ( $x$ ), but for  $x=0.80$  it is obvious that the susceptibility decreases.

The reciprocal of mass susceptibility ( $1/\chi$ ) for the system with  $x = 0.35, 0.60$  and  $0.80$  are shown in figures (4-5), (4-6) and (4-7) respectively. For manganese with concentration ( $x$ ) =  $0.31$ , we note from the straight line that the  $\text{Fe}(\text{Al}_{1-x}\text{Mn}_x)$  system is paramagnetic. It is noted that below a certain temperature all the samples with  $x = 0.35, 0.60$  and  $0.80$  behave as antiferromagnetic material and above that temperature they behave as paramagnetic material.

By replotting the mass susceptibility ( $\chi$ ) versus temperature on the same graph for the samples (with  $x = 0.35, 0.60$  and  $0.80$ ) while heating and while cooling as shown in figures (4-8), (4-9) and (4-10), a difference in the value of Neel temperature is noticed.

## **4-2 Discussion**

It has been shown in section 4-1 and figures (4-1) ,(4-2) (4-3) and (4-4), that the susceptibility measurements of the  $\text{Fe}(\text{Al}_{1-x}\text{Mn}_x)$  alloy system indicate that different magnetic phases develop as the concentration (x) of Mn changes. For  $x=0.31$  a paramagnetic phase dominates with negative paramagnetic temperature, while for  $x=0.35$  ,0.60 and 0.80 antiferromagnetic ordering appears.

There is a small increase in the susceptibility as the concentration of Mn increases, until it reaches the critical concentration at  $x= 0.35$  for the on-set of ferromagnetism as seen from Fig.(4-2).



The Neel temperature  $T_N$ , The paramagnetic temperature  $\theta_p$  and the mass susceptibility at Neel temperature were estimated from figures (4-1) up to (4-7) and tabulated in Table (4-1) .

Three magnetic phases can be shown from the figures, the ferromagnetic phase, antiferromagnetic phase and the paramagnetic phase (Fig. 4-11).

Mn conc. (x)	Neel Temp. $T_N$ (K)	Paramg. Temp. $\theta_p$ (K)	Mass Susceptibility in ( $10^{-6}$ CGS/gm) at $T_N$
0.31	—	-144 k *	3.1
0.35	335	340	838
0.60	387	393	1253
0.80	393	425	70

**Table(4-1). The magnetic parameters of  $\text{Fe}(\text{Al}_{1-x}\text{Mn}_x)$  for different manganese concentration (x) .**

\* Paramagnetic temperature ( $\theta_p$ ) cannot be calculated in temperature range ( $300 \leq k \leq 650$ ) . It is taken from previous studies .(Ref.[14]) .

The dependence of susceptibility on the Mn concentration in Fe(Al,Mn) alloy system may be due to the displacement of Fe atoms to Al sites which results in site occupation of the type B2<sub>3</sub> structure where Mn atoms occupy both Al and Fe sites. Thus the chemical formula (Fe)(Al<sub>1-x</sub>Mn<sub>x</sub>) can be written as (Fe<sub>1-y</sub>Mn<sub>y</sub>)(Al<sub>1-x</sub>Mn<sub>x-y</sub>Fe<sub>y</sub>).

This system can be seen as two sublattices: the first is (1-y){Fe(Al<sub>1-x</sub>Mn<sub>x-y</sub>Fe<sub>y</sub>)} and the second is (y){Mn(Al<sub>1-x</sub>Mn<sub>x-y</sub>Fe<sub>y</sub>)}.

In the first sublattice there exists Fe-Fe and Fe-Mn interaction in the first nearest neighbors (1 nn's) and Mn-Mn and Fe-Fe in the second nearest neighbors (2 nn's). While in the second sublattice there exist Mn-Mn and Mn-Fe interaction as (1 nn's) and Mn-Mn and Fe-Fe in the (2nn's). Due to sensitivity of Mn-Mn and Mn-Fe interaction to separation interaction [4], there might be a short-range ferromagnetic and antiferromagnetic

interaction simultaneously . Thus for lower Mn concentration  $x \leq 0.31$  , both interactions result in paramagnetic behavior of the corresponding alloys. As Mn concentration increases, the ferromagnetic interactions exceed the antiferromagnetic interactions which results in a ferromagnetically ordered samples at  $x=0.35$ . Further increase of Mn concentration, results of Mn-Mn as 1 nn's increasing, which increases the relative strength of short-range antiferromagnetic interactions. The system for  $x=0.60$  has also ferromagnetic interactions, but less than for  $x=0.35$  .

As Mn concentration increases, more strength of antiferromagnetic interactions that exceeds the ferromagnetic interactions as at  $x=0.80$  and thus decreases the mass susceptibility .

It can be concluded from Table(4-2) that the susceptibility increases for Mn concentration from  $x=0.31$  to  $x=0.60$  but then decreases for  $x=0.80$ . We can also conclude that for  $x=0.31$ , the paramagnetic temperature( $\theta_p$ ) is negative but for the other Mn concentrations ( $\theta_p$ ) is positive which is consistent with the property of atiferromagnetic materials .

Table (4-2) shows a difference in Neel temperatures for heating the samples comparable with cooling the samples . This is similar to hysteresis property. In our case heating the samples disturbs the order of the sites of the atoms in the lattice, which needs time to retain the initial stable states, since the data of the susceptibility was taken immediately for the samples after it reaches its' highest temperature. This is clear as shown in figures (4-8), (4-9) and (4-10) for  $x=0.35$ ,  $0.60$  and  $0.80$  respectively.

It can be concluded from Fig.(4-12) which is drawn in dashed lines as a guide to the eye that the maximum susceptibility increases with increasing of Manganese concentration until  $x=0.60$  , then decreases for  $x=0.80$  .

From Fig.(4-13) which is drawn in dashed lines as a guide the eye that Neel temperature increases with Manganese increasing . If we let Manganese concentration ( $x$ ) is one which means that the systems becomes Fe Mn with Al concentration is zero then  $T_N \approx 400$  K .

Also paramagnetic temperature  $\theta_p$  versus Manganese concentration ( $x$ ) is drawn in fig(4-14) . It can be seen that  $\theta_p$  is negative for  $x=0.31$ , where the sample has paramagnetic behavior , and  $\theta_p$  is positive for the other manganese concentration ( $x=0.35$  ,  $0.60$  &  $0.80$  ) . We also conclude from the graph that  $\theta_p$  increases with

increasing the Manganese concentration. Also if Manganese concentration  $x=1$ , which means that the system becomes Fe Mn without Aluminum, then  $\theta_p \approx 460$  K, which is consistent with our results .

Conce. Of Mn X	Neel Temp. $T_N(k)$ while heating	Neel Temp. $T_N(k)$ while cooling
0.35	335	314
0.60	387	369
0.80	393	374

Table (4-2). Magnetic properties of  $Fe Al_{1-x} Mn_x$  samples with different manganese concentration (x) while heating and cooling .

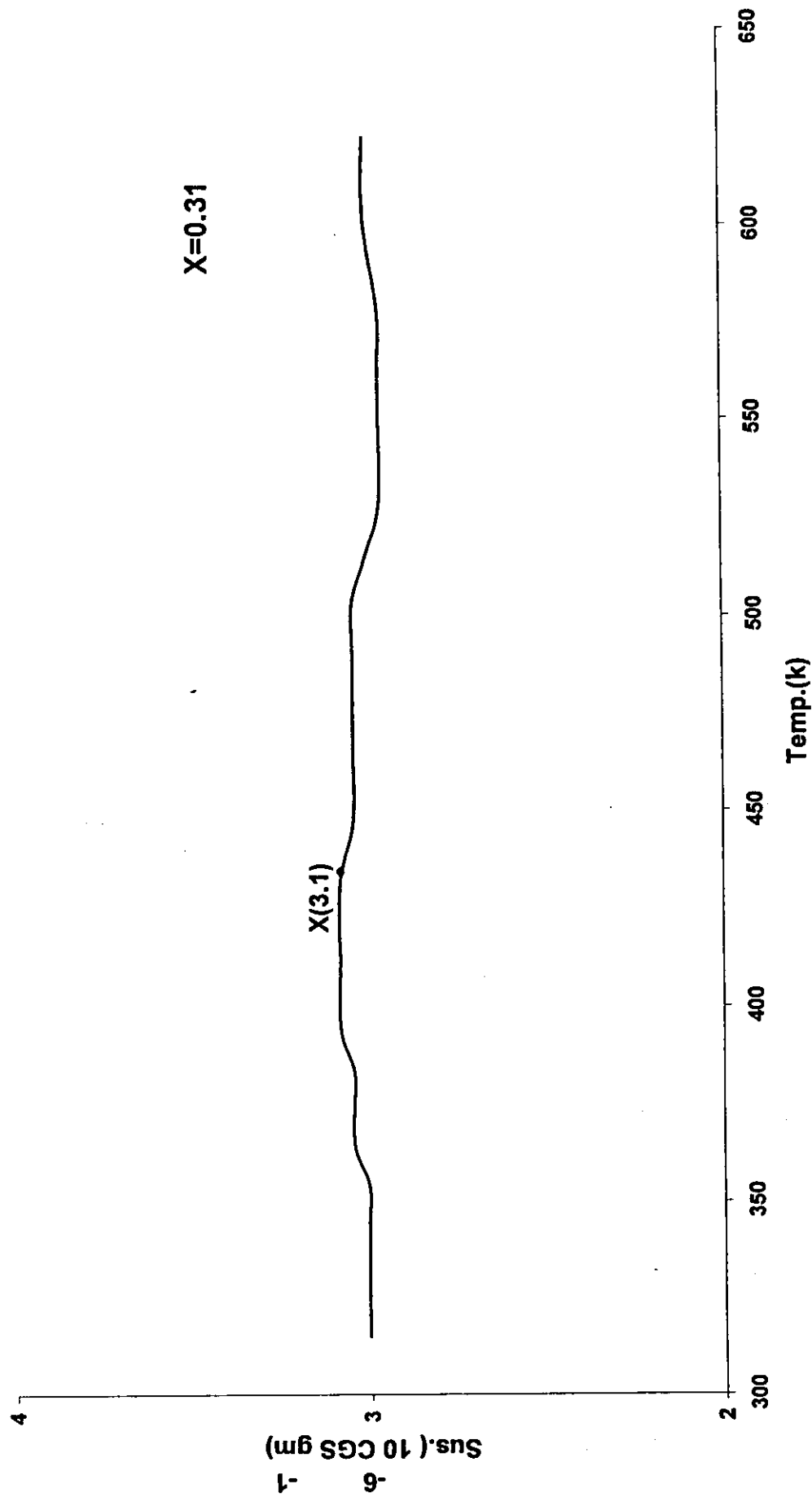
### 4-3 Summary and Conclusion

The curves of figures (4-1) ,(4-2) ,(4-3) and (4-4) show that the sample for  $x=0.31$  is paramagnetic , and the samples for  $x=0.35$ , 0.60 and 0.80 are of coexistence of ferromagnetic and antiferromagnetic ordering .

The susceptibility of the paramagnetic sample for ( $x=0.31$ ) is found to obey a Curie-Weiss law with a negative paramagnetic temperature ( $\theta_p$ ) = -144K. But the susceptibility of the other samples (for  $x=0.35, 0.60$  and  $0.80$ ) show antiferromagnetic properties with different Neel temperature ( $T_N$ ) and positive paramagnetic temperature ( $\theta_p$ ). Neel temperature ( $T_N$ ) and Paramagnetic temperature ( $\theta_p$ ) are very close to each other,  $\theta_p \geq T_N$ , but are rarely equals.

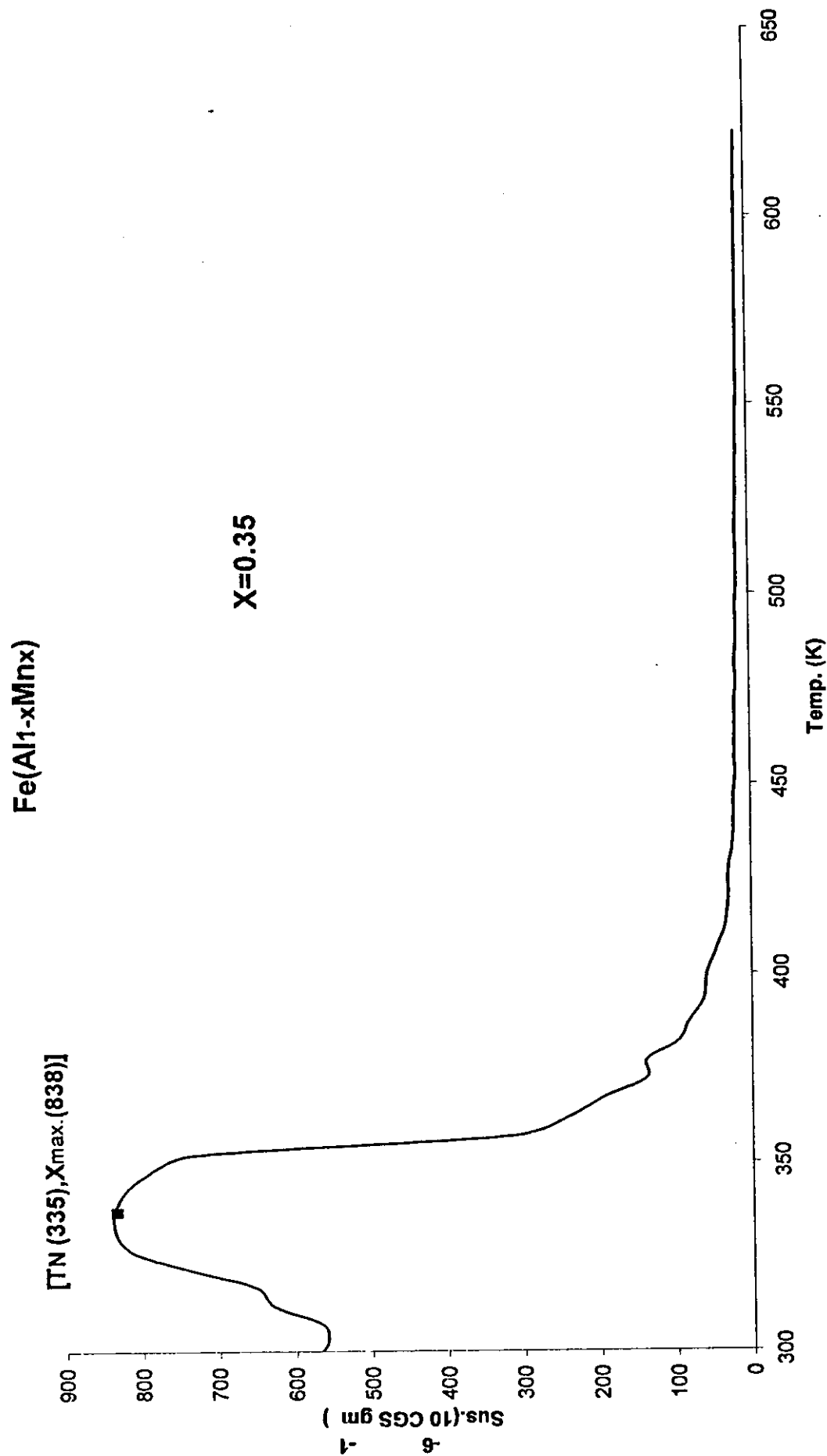
The susceptibility of the Fe ( $Al_{1-x}Mn_x$ ) system increases with increasing the concentration of manganese atoms until saturation is achieved.

It is noticed clearly from figures (4-8), (4-9) and (4-10) that there is a difference in the maximum susceptibility and Neel temperature of the Fe ( $Al_{1-x}Mn_x$ ) system, while heating compared to that while cooling.

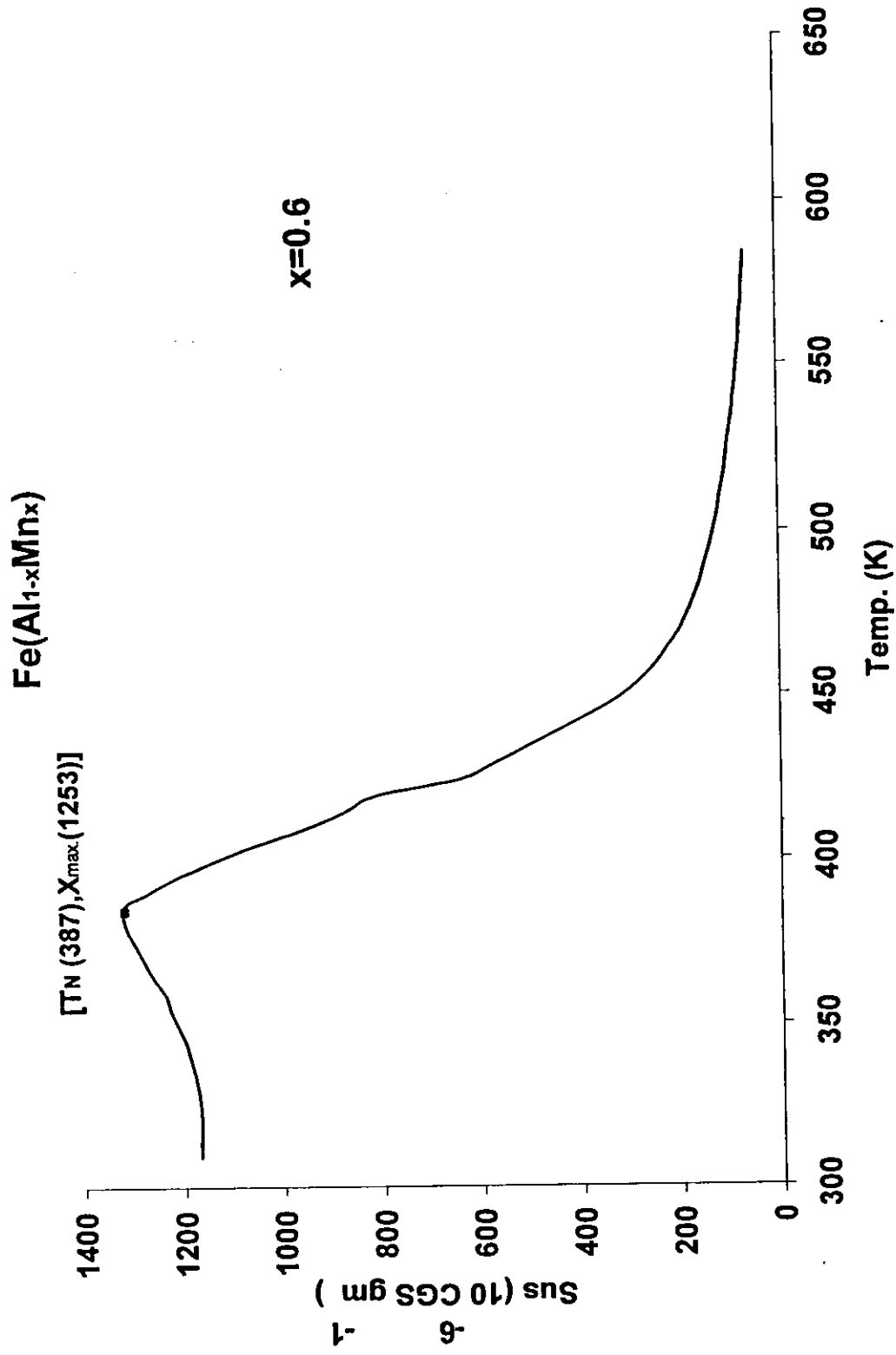


**Fig(4-1) : Variation of susceptibility with temperature  $T$  for  $\text{Fe}(\text{Al}_{1-x}\text{Mn}_x)$  with  $x=0.31$  .**

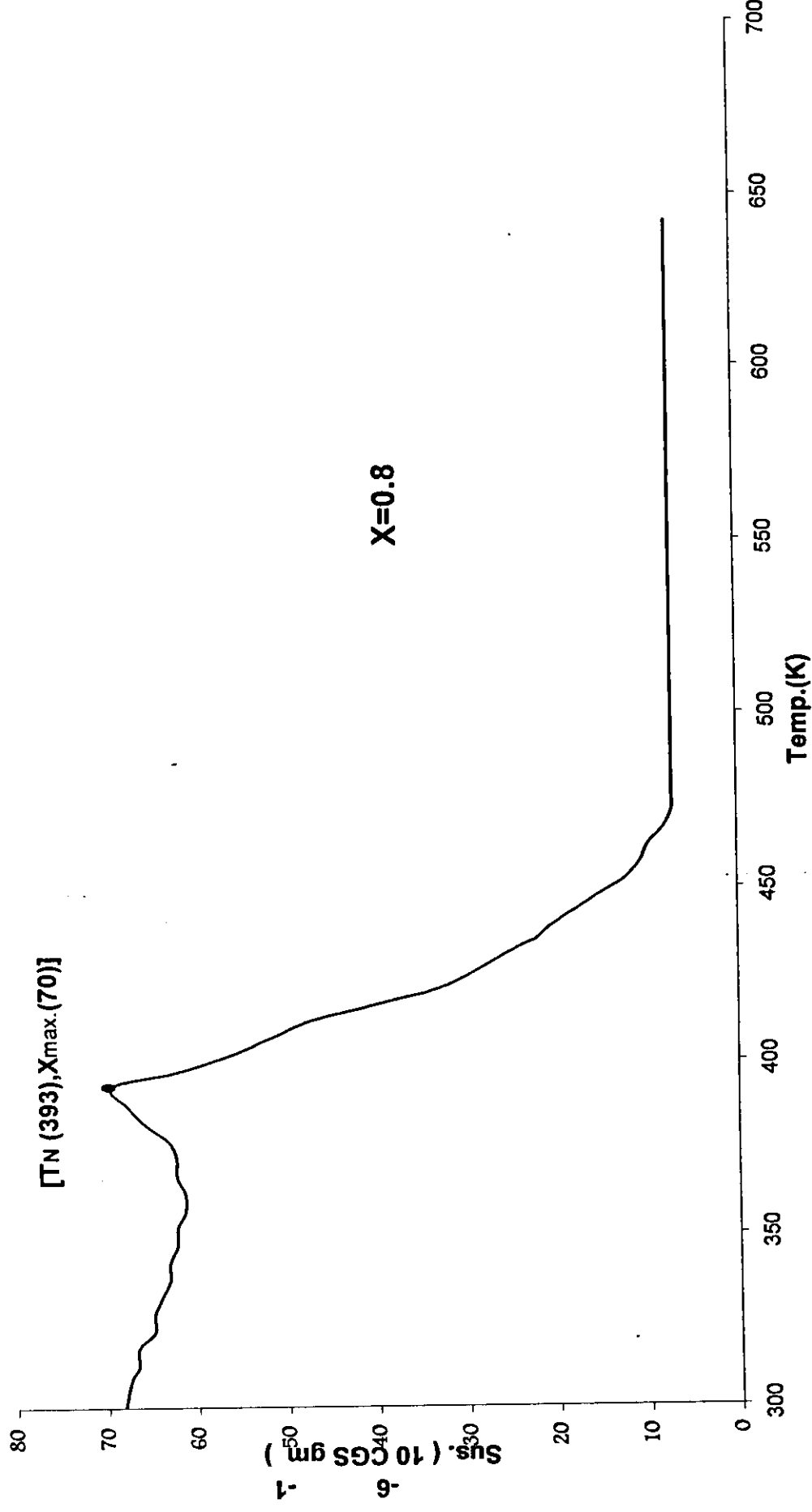




**Fig(4-2) : Variation of susceptibility with temperature  $T$  for  $\text{Fe}(\text{Al}_{1-x}\text{Mn}_x)$  with  $x=0.35$ .**



**Fig(4-3) : Variation of susceptibility with temperature *T* for Fe(Al<sub>1-x</sub>Mn<sub>x</sub>) with x=0.60 .**



**Fig(4-4) : Variation of susceptibility with temperature  $T$  for  $\text{Fe}(\text{Al}_{1-x}\text{Mn}_x)$  with  $x=0.80$  .**

$\text{Fe}(\text{Al}_{1-x}\text{Mn}_x)$

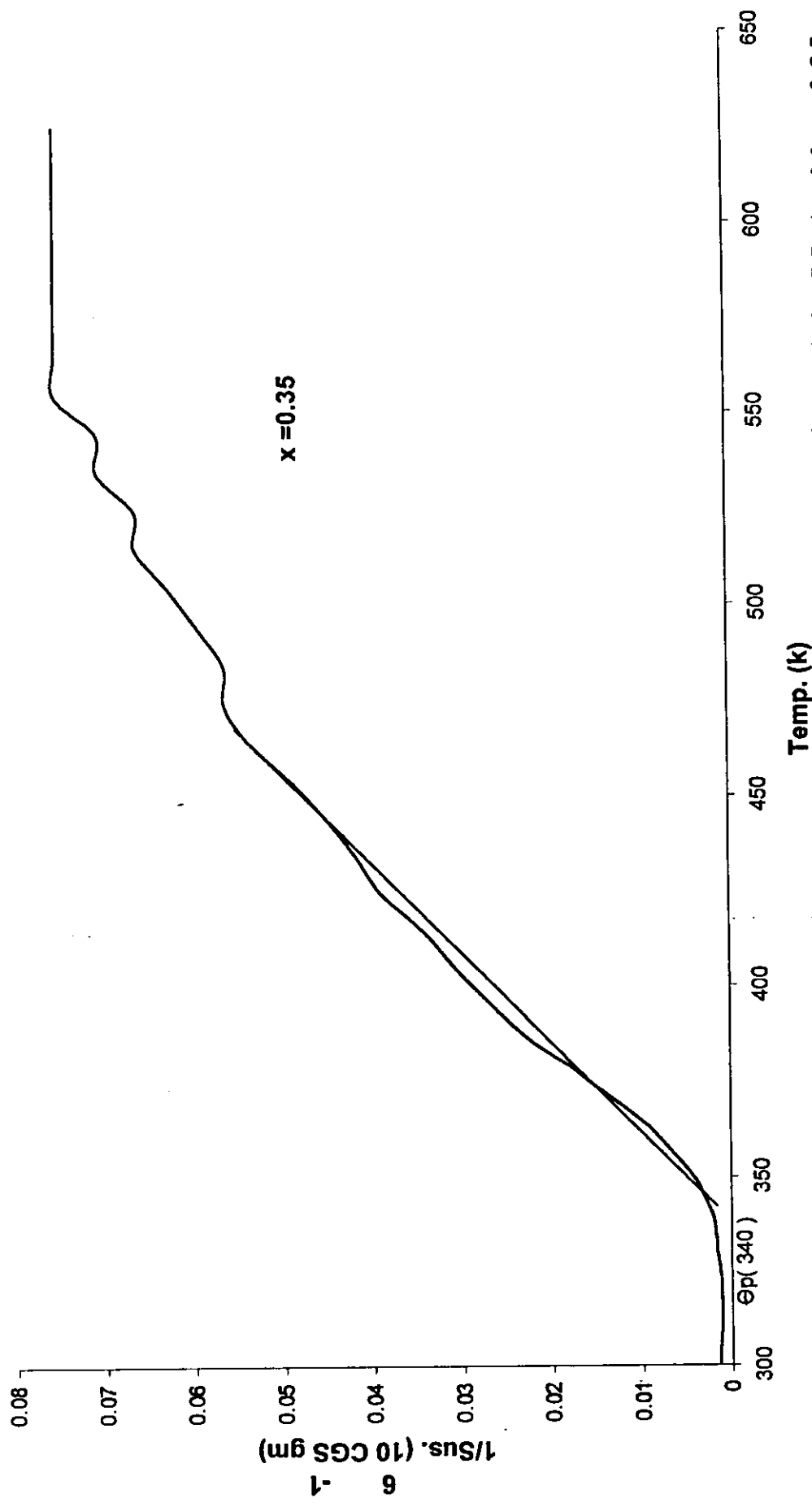


**Fig.(4-5): Variation of reciprocal of susceptibility ( $1/\chi$ ) with temperature  $T$  for  $\text{Fe}(\text{Al}_{1-x}\text{Mn}_x)$  with  $x=0.35$ .**

# $\text{Fe}(\text{Al}_{1-x}\text{Mn}_x)$

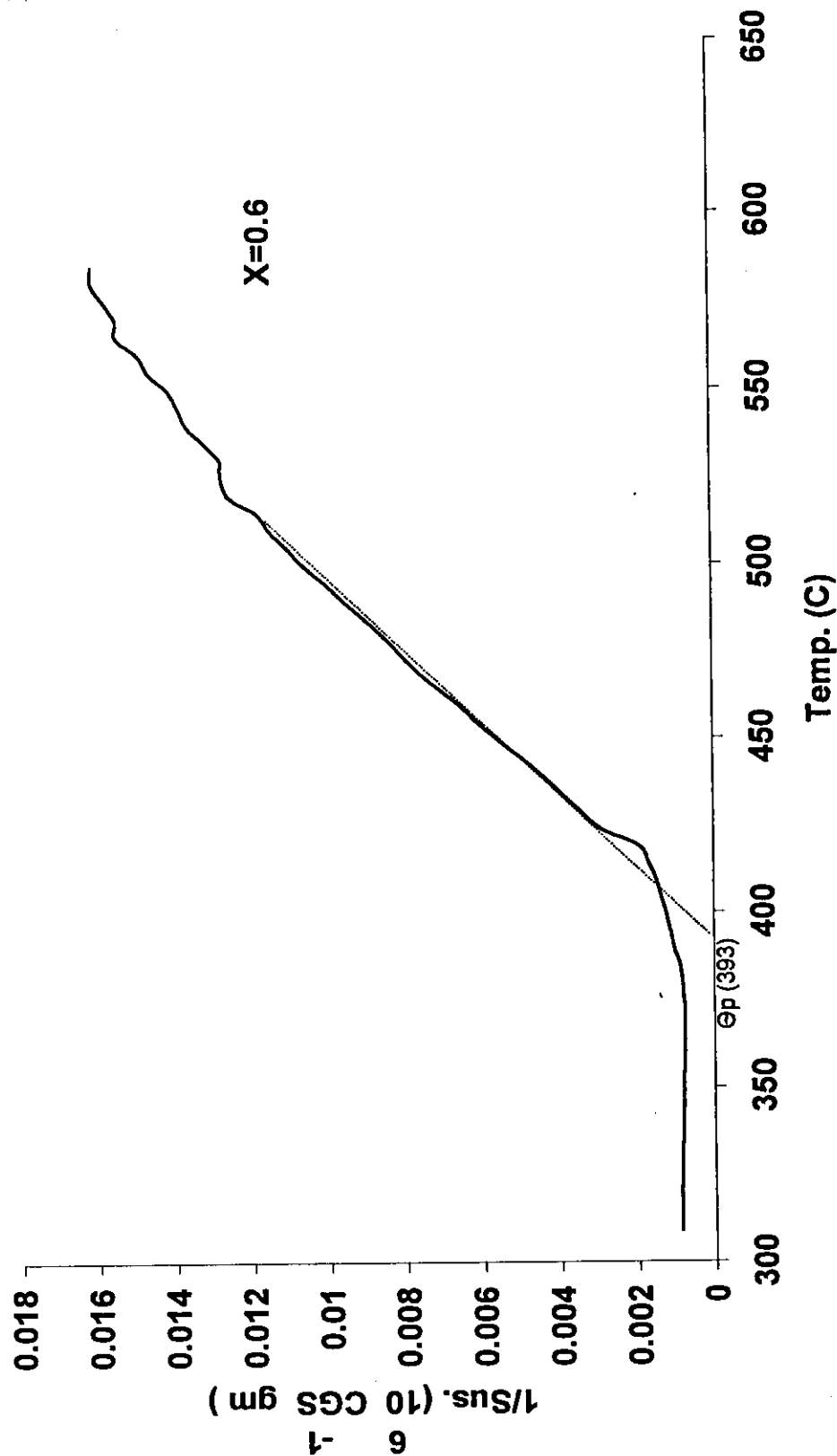


**Fig.(4-6): Variation of reciprocal of susceptibility ( $1/\chi$ ) with temperature  $T$  for  $\text{Fe}(\text{Al}_{1-x}\text{Mn}_x)$  with  $x=0.60$ .**

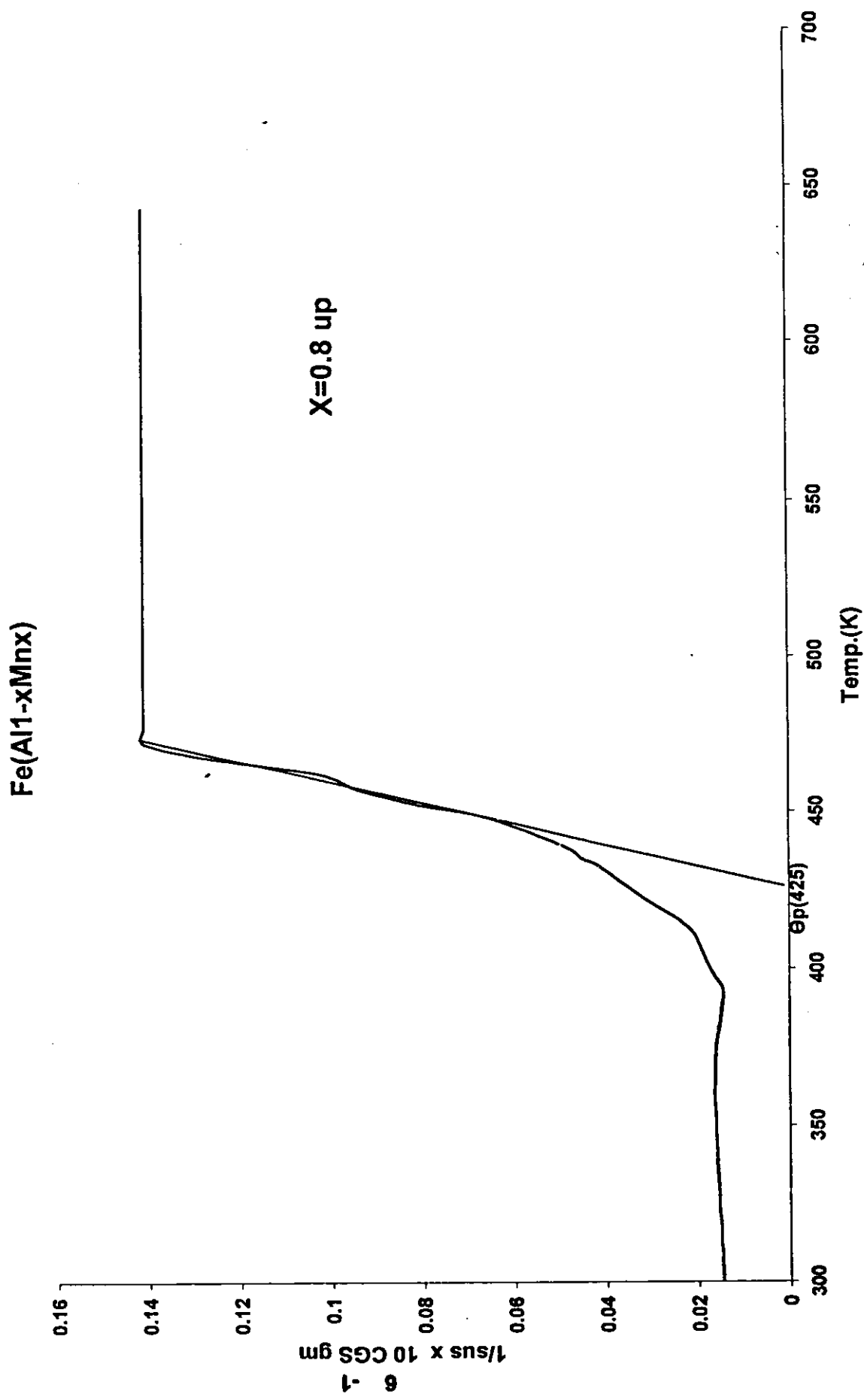


**Fig.(4-7): Variation of reciprocal of susceptibility ( $1/\chi$ ) with temperature  $T$  for  $\text{Fe}(\text{Al}_{1-x}\text{Mn}_x)$  with  $x=0.80$  .**

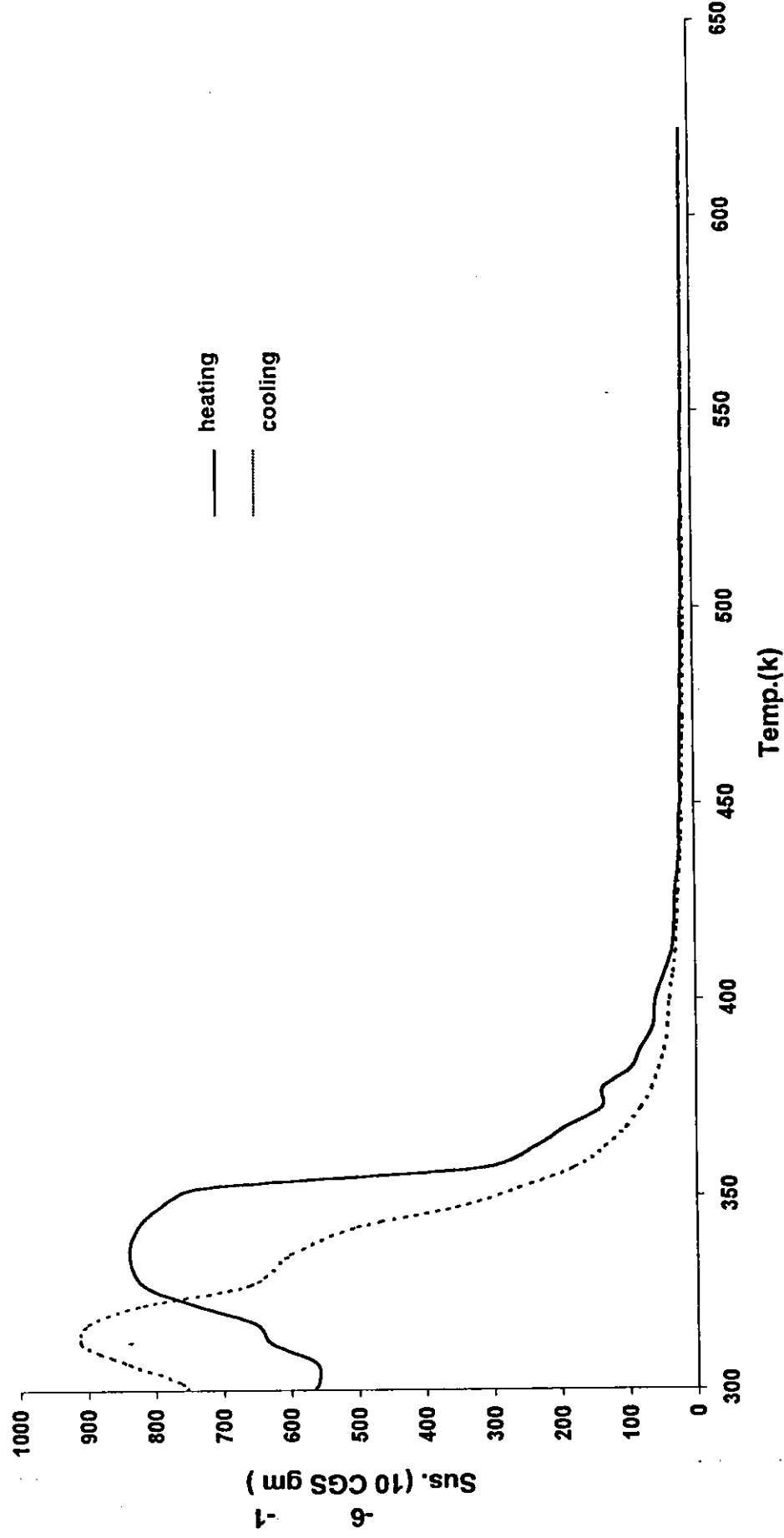


**Fig.(4-8) Susceptibility versus temperature while heating and cooling for Fe(Al<sub>1-x</sub>Mn<sub>x</sub>) with x=0.35 .**

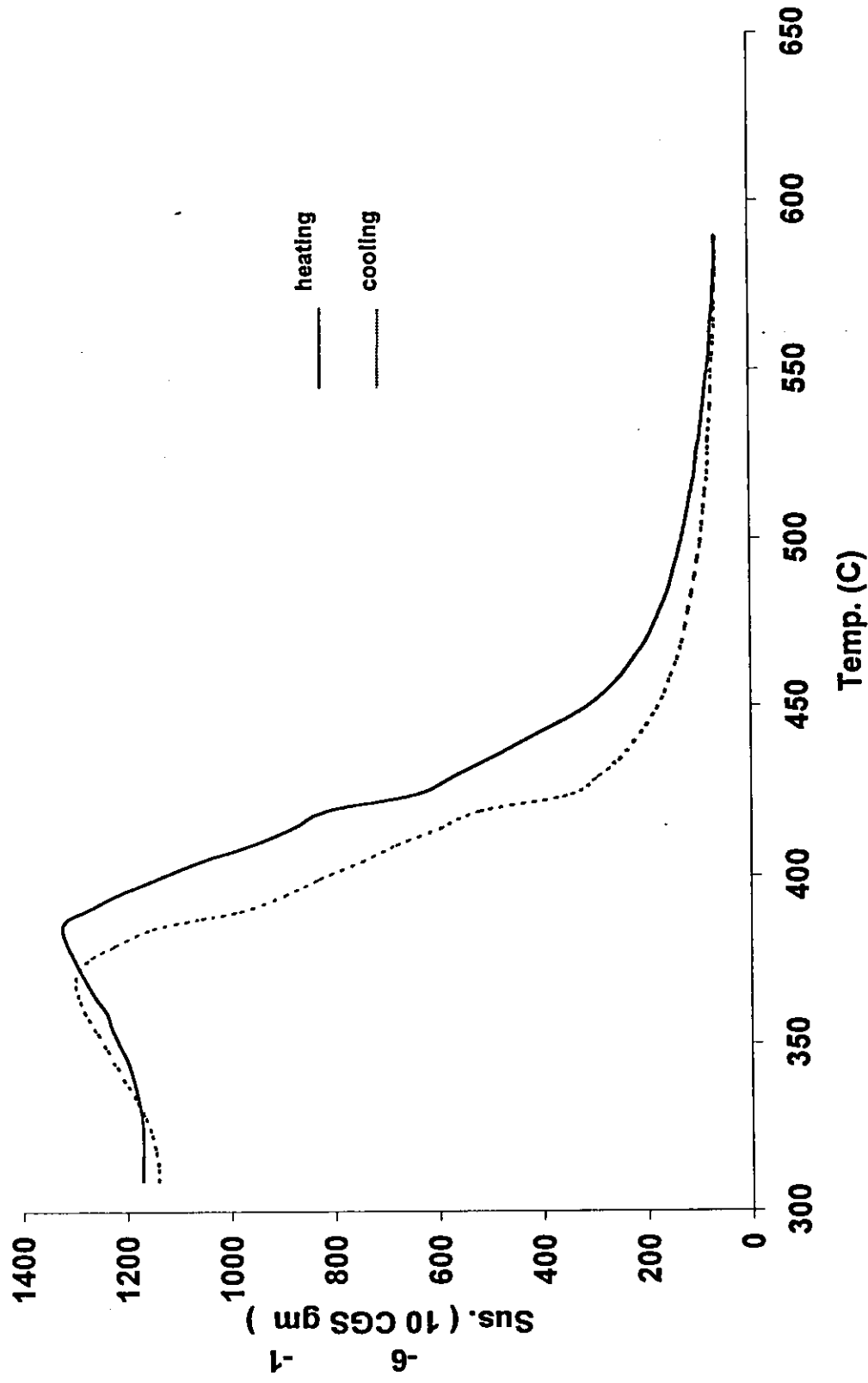
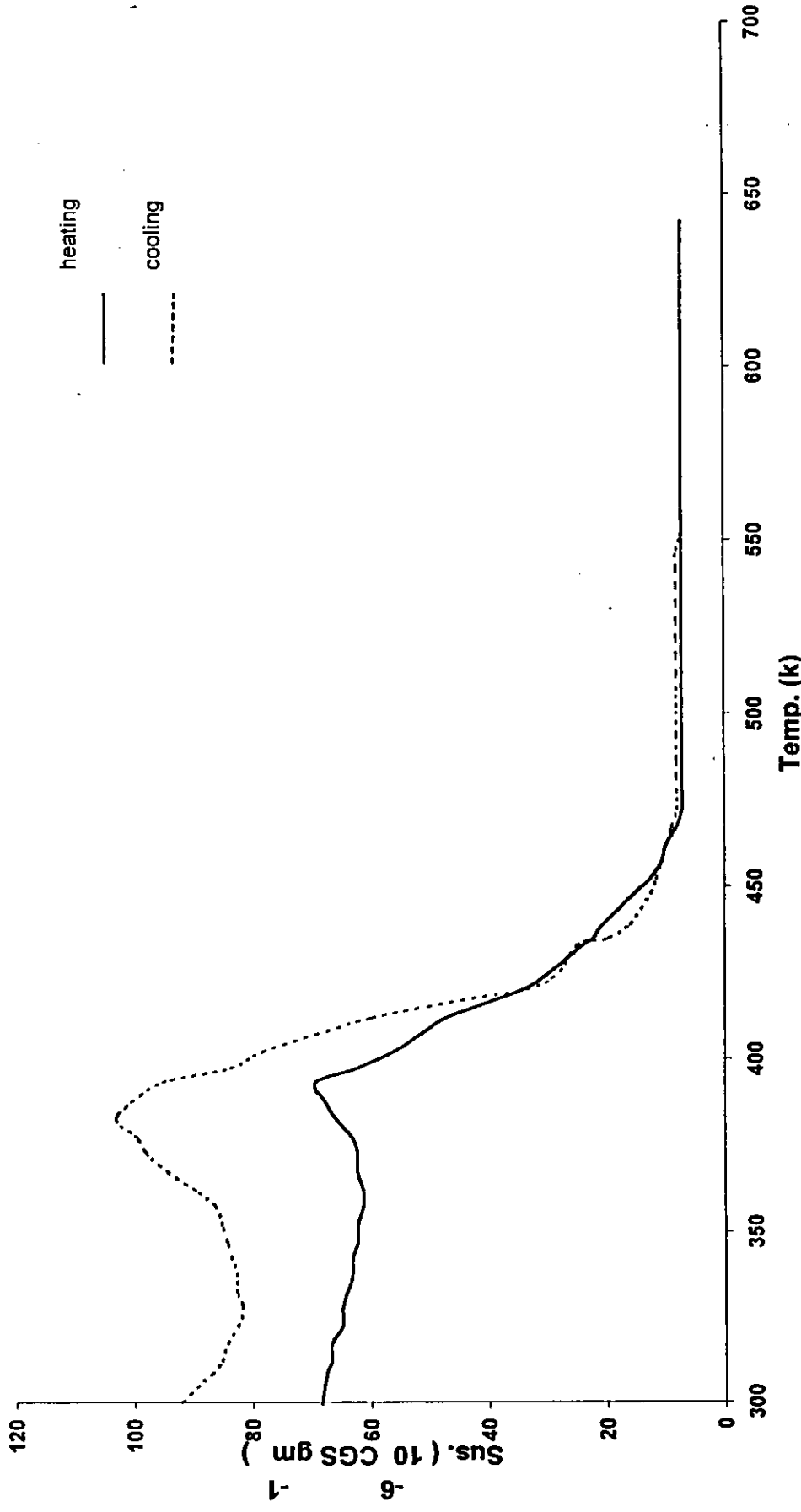
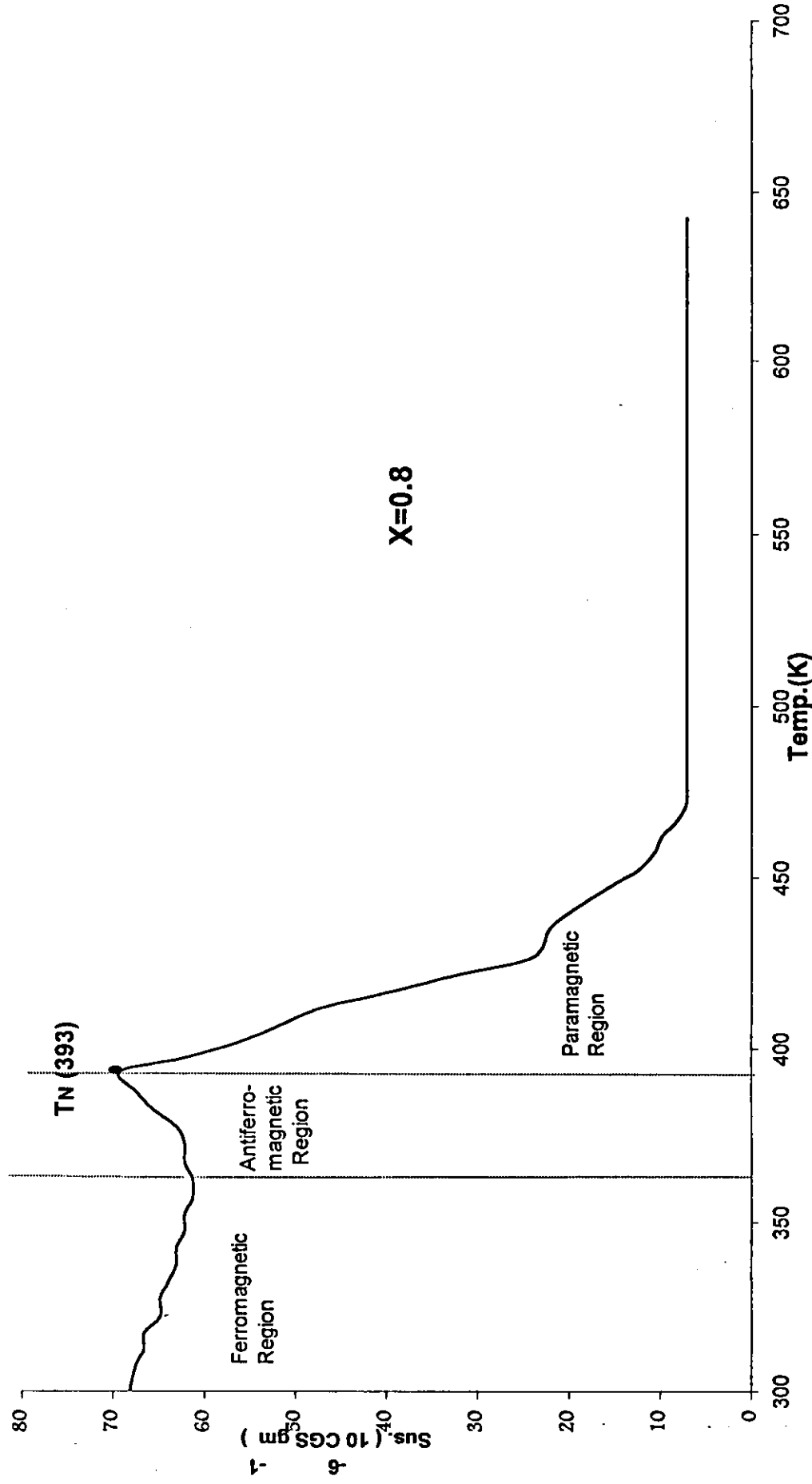
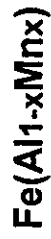


Fig.(4-9) Susceptibility versus temperature while heating and cooling for  $\text{Fe}(\text{Al}_{1-x}\text{Mn}_x)$  with  $x=0.60$ .

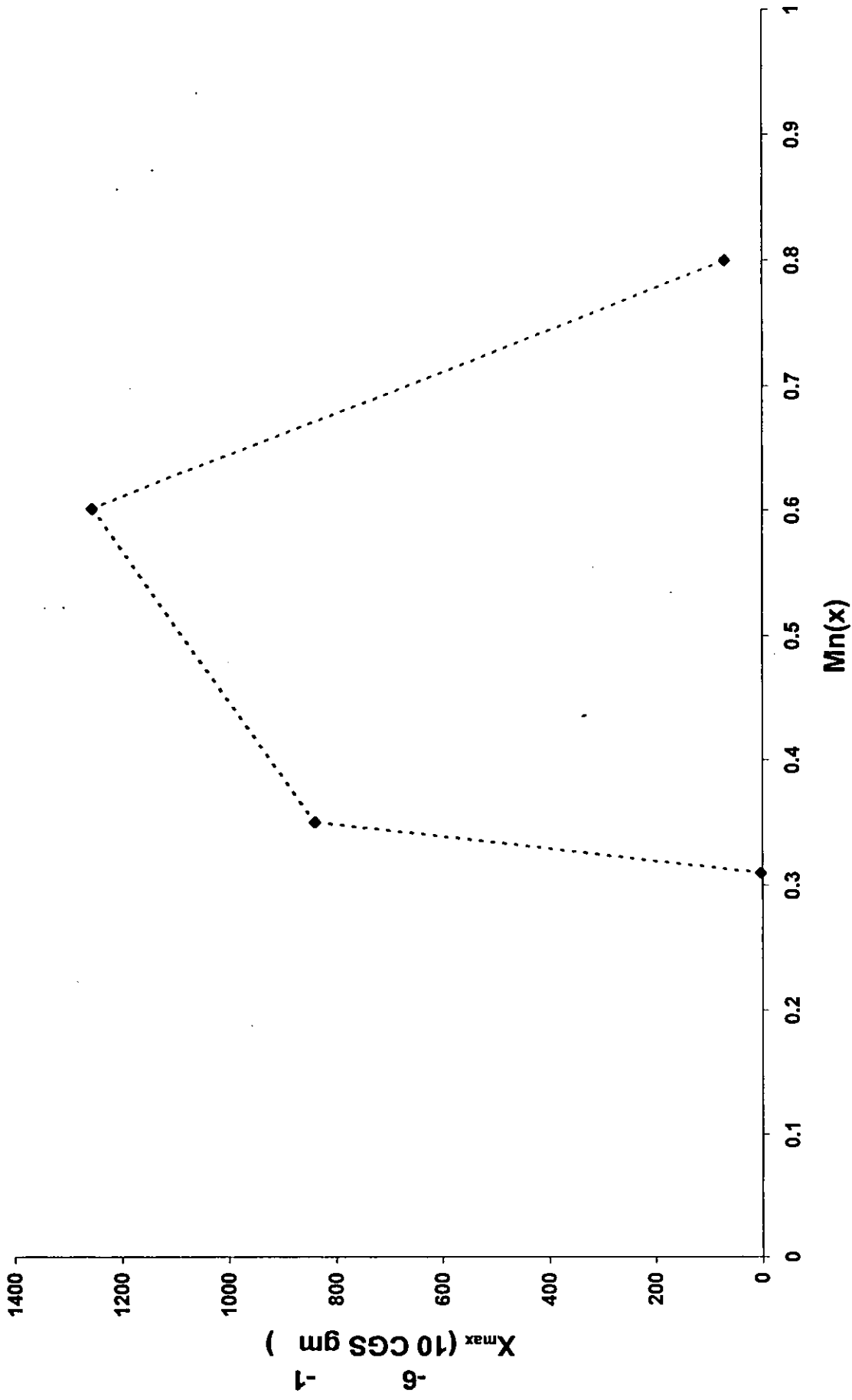




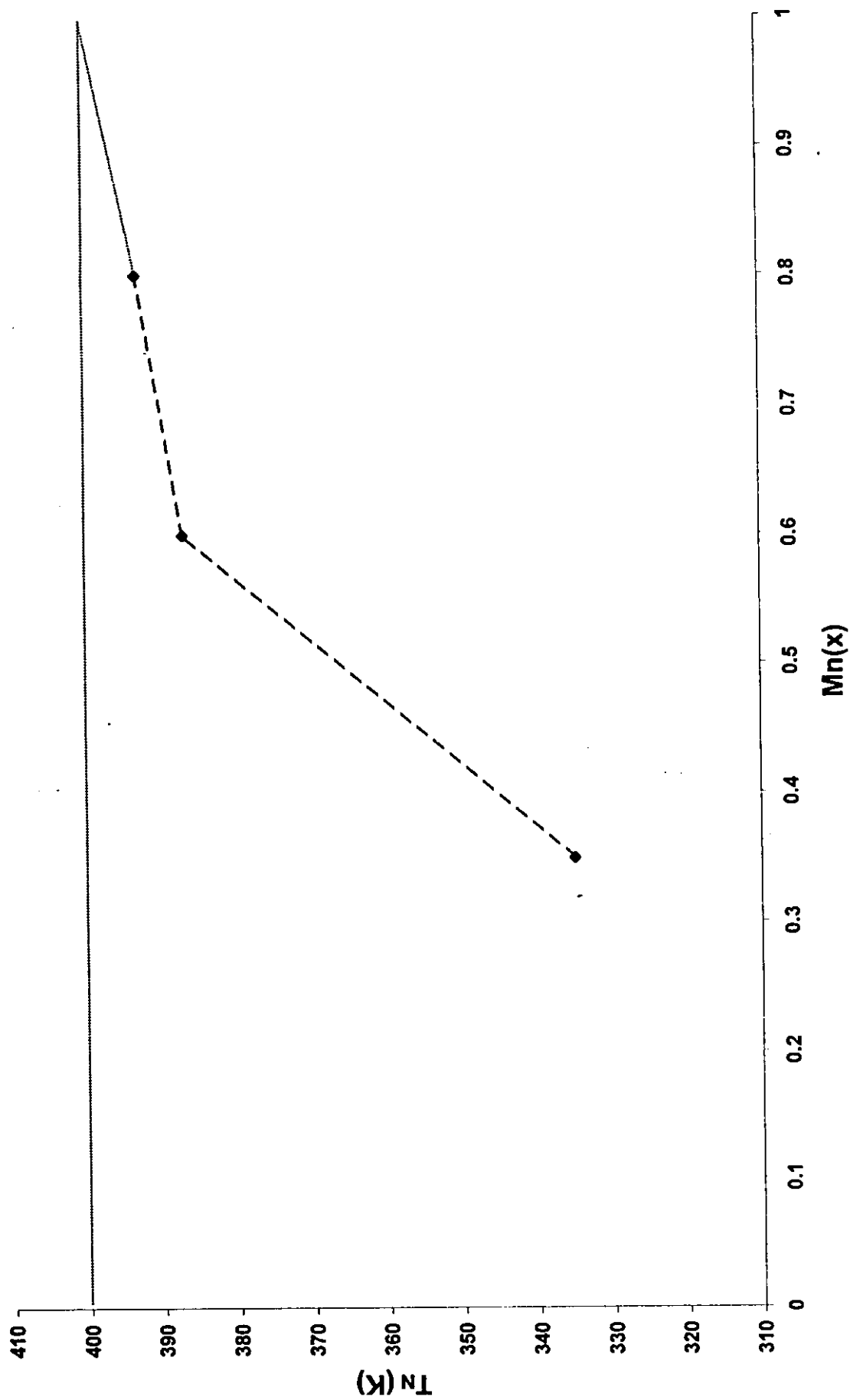
*Fig.(4-10) Susceptibility versus temperature while heating and cooling for Fe(Al<sub>1-x</sub>Mn<sub>x</sub>) with x=0.80 .*



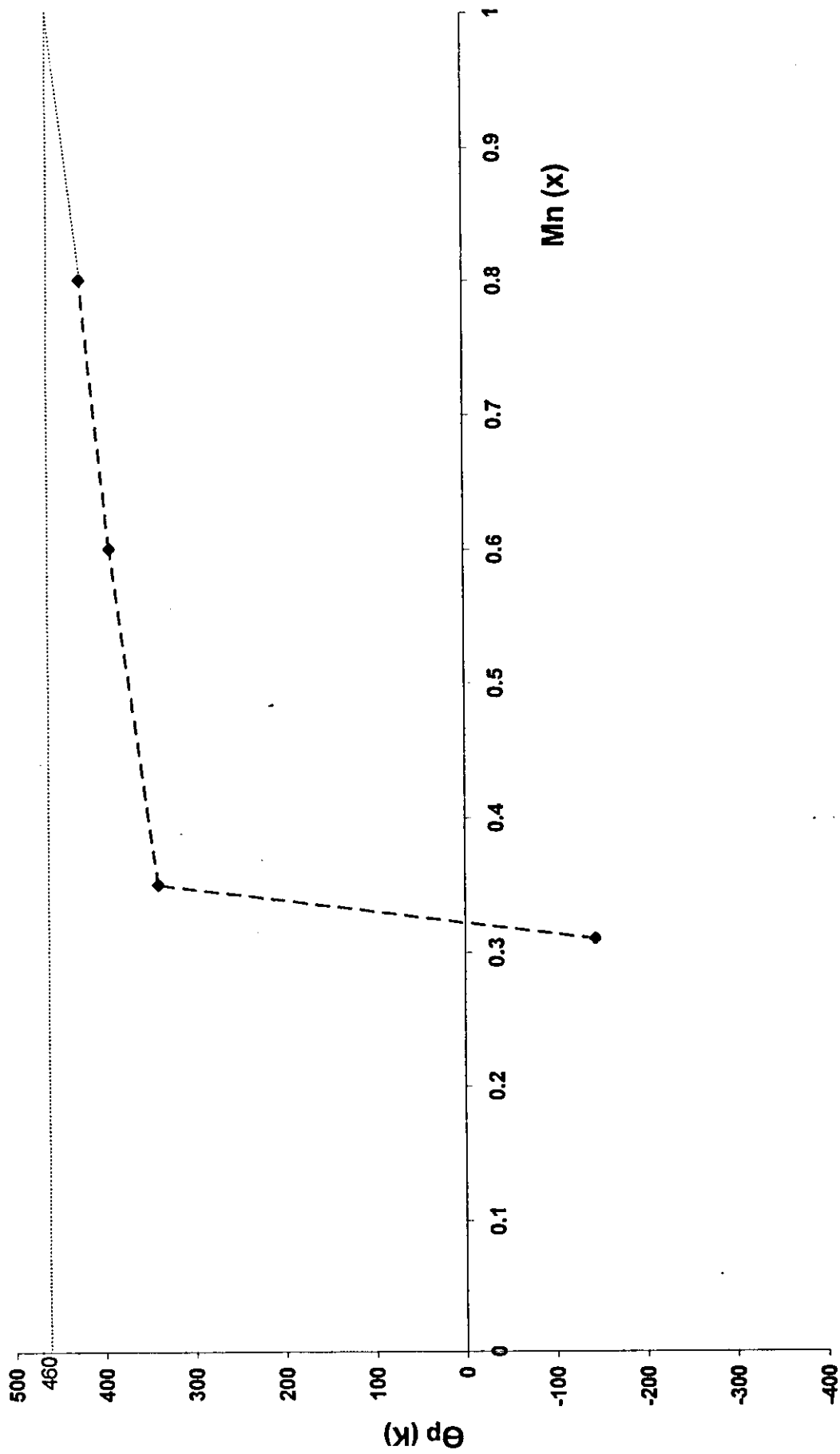
**Fig.(4-11) Variation of susceptibility with temperature for  $\text{Fe}(\text{Al}_{1-x}\text{Mn}_x)$  with  $x=0.8$ , showing three different phases (ferromagnetic, antiferromagnetic and paramagnetic regions) .**



**Fig(4-12):** *Variation of maximum susceptibility with manganese concentration of the system  $\text{Fe}(\text{Al}_{1-x}\text{Mn}_x)$   
Dashed lines are drawn through data points a guide to the eye .*



**Fig(4-13): Variation of Neel temp. with manganese concentration .**  
*Dashed lines are drawn through data points a guide to the eye .*



**Fig(4-14) Paramagnetic temp.  $\Theta_p$  versus manganese concentration .**  
*Dashed lines are drawn through data points a guide to the eye .*

## **References**

- [1] M. J. Benus. H. Herr and A. J. P. Meyer, J. phys.  
,F5(1975) 2138.
- [2] D. E. okpalugo, J. G. Booth and C. A. France ,J. phys.  
,F15(1985) 681.
- [3] Y. Hamam , M. R. said , J. shobak ,and I. Abu-  
Aljarayesh, Mu'tah J. For Research Studies ,  
11(1996) 4 .
- [4] D. E. okpalugo , and J. G. Booth , J. phys. Met. phys.  
,F15(1985) 2025 .
- [5] I. Abu-Aljarayesh, M. R. said and Y. A. Hamam, Solid  
st. Com., 99(1996)567 .
- [6]William F. Smith, "Foundations of Mater. Science and  
Engineering" (McGraw-Hill, Inc. International) 1993 .
- [7] G. Mills and J.G Booth, J. Magn. Matter, 119(1993)30.

547644

- [8] E. Kim and S. Yoon, J. Korean Inst. , 25(1987)711 .
- [9] M.A Kobelssi, Q.A. pankhurst ,S. suharan and M. F. Thomas, J. phys. C: cond . Matter , 2(1990) 4895 .
- [10] A. S. Saleh, R. M. Mankikar , S. Yoon , D. E. okpalugo and J. G. Booth, J. Appl. phys. ,57(1985) 3241 .
- [11] K. Y. Ko and S. Yoon, J. Korean Inst. ,27(1989)1008.
- [12] I. Abu-Aljarayesh , S. Mahmood and A. F. Lehlooh, J. Magn. Magn. Matter, 140(1995) 65 .
- [13] I. Omari , A.S. Saleh and S.H. Mahmood, J. Magn. Matter, 78 (1989) 138 .
- [14] I. Abu-Aljarayesh, S. Al-Kateep, M. R. Said, J. Magn. Magn. Matter., 185(1998) 220-224 .
- [15] R. Boca/Coordination Chemistry Reviews 172(1998)167-283 .

- [16] J. Crangle , "The magnetic Properties of Solids" ,  
(Edward Arnold, London ) 1977 .
- [17] N. W. Aschroft and N. D. Mermin, "Solid State  
Physics", (Holt-Saunders,Tokyo) 1976 .
- [18] Derek Craik, "Magnetism Principles and  
Application", (J.Willey & Sons,New York) 1995 .
- [19] C. Kittel, "Introduction to Solid State Physics",  
(J.Willey & Son, United States) 1976 .
- [20] J. G. Booth "Ferromagnetic Materials" Ed(S),E. P.  
Wohlfarth and K. H. J. Buschow , V01.4 (North-  
Holland, New Yourk)(1988) 211 .
- [21] MS2 Magnetic Susceptibility System Manual,  
Bartington Instruments, Witeney ,Oxford, U.K.,  
(1998) .